ANTITUMOR EFFECTS OF MODULATED ELECTRO-HYPERTHERMIA IN 4T1 TRIPLE-NEGATIVE BREAST CANCER MODELS

PhD thesis

Lea Danics PharmD

Doctoral School of Theoretical and Translational Medicine

Semmelweis University

Supervisor: Péter Hamar, MD, DSc

Official reviewers: Attila Marcell Szász, MD, PhD
Gábor Pozsgai, MD, PhD

Head of the Complex Examination Committee: Janina Kulka, MD, DSc

Members of the Complex Examination Committee: Mihály Újhelyi, MD, PhD
Dániel Sándor Veres, MD, PhD

Budapest
2021

Table of content

List of Abbreviations

AEMF	-	Alternating Electromagnetic Field
AM	-	Amplitude Modulation
ANOVA	-	Analysis of Variance
cC3	-	Cleaved Caspase-3
CHPP	-	Continuous Hyperthermic Peritoneal Perfusion
DAB	-	3,3'-diaminobenzidine
DMSO	-	Dimethyl Sulfoxide
ECG	-	Electrocardiogram
EMF	-	Electromagnetic Field
ER	-	Estrogen Receptor
H&E	-	Hematoxylin and Eosin
HER2	-	Human Epidermal Growth Factor Receptor 2
HIFU	-	High-Intensity Focused Ultrasound
HIPEC	-	Hyperthermic Intraperitoneal Chemotherapy
HSE	-	Heat Shock Element
Hsf-1	-	Heat Shock Factor-1
Hsp	-	Heat Shock Protein
HSR	-	Heat Shock Response
HT	-	Hyperthermia
IHC	-	Immunohistochemistry
IVIS	-	In Vivo Imaging System
mEHT	-	Modulated Electro-hyperthermia
PR	-	Progesterone Receptor
RF	-	Radiofrequency
SAR	-	Specific Absorption Rate
SEM	-	Standard Error of the Mean
TDR	-	Tissue Destruction Rate
TNBC	-	Triple-Negative Breast Cancer
WBH	-	Whole Body Hyperthermia

1. Introduction

1.1. Breast cancer

Cancer of the breast is one of the most frequent malignancy among women [1]. There are over two million new cases and over half a million death dedicated to malignancies of the breast every year worldwide, and the global incidence is still rising [1]. Breast cancers are very heterogeneous, they differ in histological origin (e.g. ductal or lobular carcinomas) molecular characteristics (e.g. mutational status, hormone receptor and human epidermal growth factor receptor 2 (HER2) status, Ki67 status, etc.) and clinical behavior [2]. These features determine the disease phenotype, progression and outcome, as well as the therapeutic options. In this regard, several classifications have been made on the basis of histological and molecular characteristics of breast cancers to improve therapeutic decisions and predict the progression and outcome of the disease [2].

The main histological subtypes of breast malignancies are the ductal and the lobular carcinomas, i.e. cancer arising from the epithelial cells lining the ducts or the terminal duct lobular units [2]. As far as the malignant cells do not break through the basal membrane, the malignancy is referred as carcinoma *in situ* or preinvasive carcinoma [2]. Early-stage, non-metastatic breast cancers are considered nowadays as curable diseases, as ~70-80% of the patients can be cured thanks to the improvements in multimodal anti-cancer therapies, namely surgery with radiotherapy and/or chemotherapy or targeted therapy [2]. However, invasive and metastatic breast malignancies – frequently referred to as advanced breast cancers – still remain incurable diseases with a median survival time of ~3 years and often lead to the death of the patient [2,3]. Thanks to the developments in breast cancer research, it has become clear, that not just histological, but other features – mutational status, gene amplifications, gene expression profile – also have crucial implications for successful therapy [2]. In 2000 Perou and Sorlie introduced the intrinsic subclassification of breast malignancies, which is based on a 50-gene expression signature (PAM50) (Figure 1.) [4]. This subclassification defines six intrinsic subtypes, that are: Luminal A, Luminal B, Claudin-low, Basal-like and Normal-like breast cancers [4]. In clinical practice a surrogate intrinsic subclassification is currently used to support the therapeutic decision, which is based on histological features and expression profiles of key proteins in breast cancers, like estrogen receptor (ER),

progesterone receptor (PR), human epidermal growth factor receptors 2 (HER2) and Ki67 proliferation marker (Figure 1.) [2]. These surrogate intrinsic subtypes of breast cancers are the Luminal A-like, Luminal B-like HER2$^-$, Luminal B-like HER2$^+$, HER2-enriched and Triple-negative breast cancers [2].

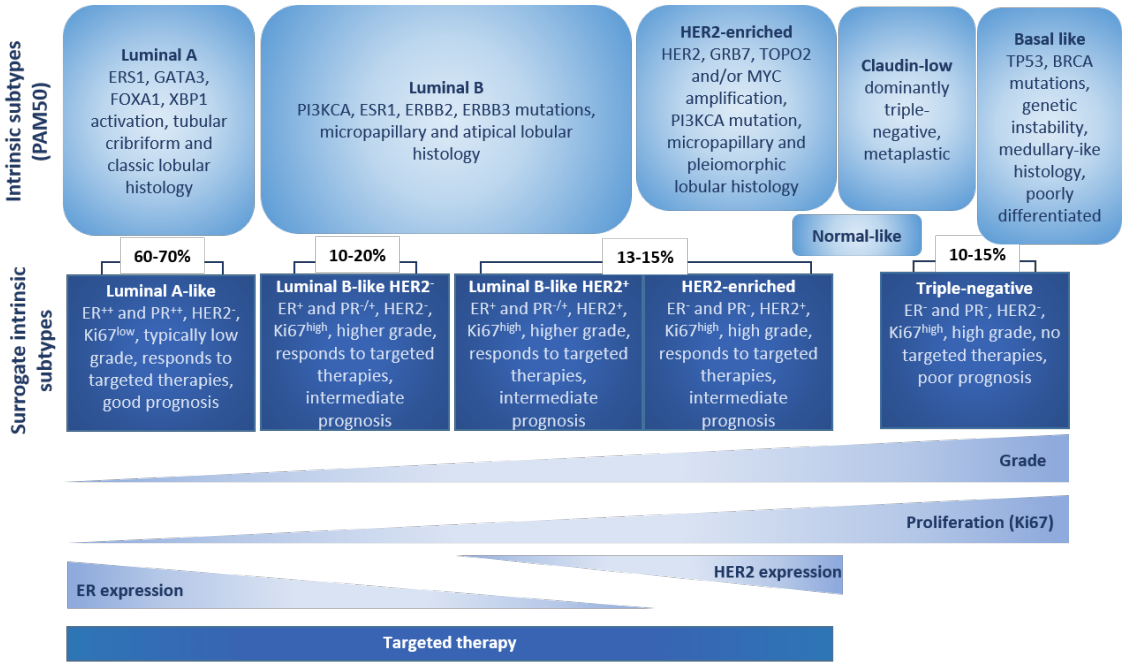

Figure 1. Molecular subclassifications of breast malignancies The intrinsic subclassification of breast cancers is based on the expression signature of 50 genes (PAM50). The six intrinsic subtypes were defined by Perou et al. in 2000 the most characteristic features (e.g. gene amplifications, activations and mutations, histology) of the subtypes are summarized in the Tables. The normal-like subtype has an expression profile very similar to normal breast tissue, due to low tumor cellularity. Surrogate intrinsic subclassification is more practical and provides strong support in therapeutic decision as it is based on histological and immunohistochemical detection of key proteins, which can serve as therapeutic targets (estrogen receptor (ER), progesterone receptor (PR), human epidermal growth factor receptor 2 (HER2)) or which can predict disease progression (proliferation marker Ki67). The surrogate intrinsic subclassification of breast cancers is widely used in clinical practice [2].

1.1.1. Triple negative breast cancer

Triple negative breast cancer (TNBC) is one of the surrogate intrinsic subtypes of breast cancers, defined by the lack of estrogen-, progesterone-receptors and HER2 expression [5,6]. Besides this, typical features are the high proliferation index (Ki67 status), high grade, invasive histology and poor prognosis [2,5,6]. TNBC accounts for 10-17% of all breast carcinomas, however it is more frequent among young patients (< 50 years) and African-American women [7]. Due to its aggressiveness, the risk of recurrence peaks between the first to third years following therapy and the majority of deaths occur in five years [6,7]. Another major problem is, that there is no targeted therapy available for TNBC patients, since the tumors do not express any of the ER, PR or HER2 receptor proteins [2,5,6]. Worth to note that new targeted therapies are intensively investigated in TNBC [8] and it seems that currently emerging immune checkpoint inhibitors show encouraging results in TNBC patients according to recent clinical trials [9]. For TNBC patients the only available standard, guideline-approved systemic treatment option still is cytotoxic chemotherapy [3,10,11]. According to the St. Gallen guideline, patients with triple-negative breast cancer are recommended to receive cytotoxic chemotherapy containing an anthracycline and a taxane [11]. These drugs are not selective, are highly toxic and cause a lot of side effects which make them poorly tolerable by the patients [12,13]. Furthermore, both anthracyclines and taxanes can cause long-term side effects, like cardiotoxicity and neurotoxicity, which strongly affect the quality of life of the patients and sometimes even lead to their non-cancer-related death [14]. Some studies suggest that TNBCs respond better to chemotherapy than other breast cancers, however their prognosis remains poor, due to the extremely aggressive phenotype [15,16]. Based on all these aspects, new therapeutic options or complementary therapies are urgently needed to improve disease outcome and survival of TNBC.

1.1.2. 4T1 and 4T07 mouse isograft models of triple negative breast cancer

For modeling and investigating the human TNBC disease in preclinical settings, several small animal models were established [17]. One of these is the 4T1 mouse model, which is widely used in preclinical research [17,18]. 4T1 cells were isolated from a spontaneously arisen 410.4 mammary carcinoma of a female BALB/c mouse by Fred Miller et al. and selected from the other three sublines (4T07, 168FARN and 67NR) based on its natural resistance to 6-thioguanine [19]. 4T1 cells have a triple-negative phenotype

(no expression of estrogen-, progesterone-receptors or HER2) [20] and they are strongly tumorigenic and invasive with a very high metastatic ability to lymph nodes, blood, liver, lung, brain and bone [21,22]. Inoculating 4T1 cells into syngeneic BALB/c mice (isograft) provides a suitable, immunocompetent model for triple-negative breast cancer, since the molecular and pathophysiological characteristics are very similar to those of the human disease [20,22]. The 4T07 mouse model is also a commonly used preclinical model for TNBC. 4T07 is a 6-thioguanine-, ouabain-resistant variant of 410.4 mammary carcinoma, which has also highly tumorigenic triple-negative phenotype such as 4T1, however it has poor metastatic ability [19,23].

1.2. Hyperthermia in oncology

Hyperthermia in oncology refers to the use of therapeutic heat energy to treat various malignancies [24]. This treatment modality is considered as a complementary oncology treatment and is always used in combination with other therapies, such as chemo-, radio- or targeted and other biological oncotherapies. The intake of the applied energy usually results in an elevated intra- and peritumoral temperature at the treated site in the range of 40-48 °C, which is maintained for one or more hours [25]. The energy absorption and concomitant heat generation at the treated site can cause various biological effect, e.g. direct cell stress and interruption of the mitotic cycle at metaphase (in the range of 39-40°C), irreversible cell destruction (over 40°C), inhibition of microcirculation (over 41°C) and cell death (above 42°C) [26]. Besides these direct antitumor effects of hyperthermia, it also has favorable properties as complementary treatment, working as a radio-sensitizer [27] and drug uptake enhancer [28,29]. According to the dimensions of the treated site, there are three main clinical applications of hyperthermia: local, regional or whole-body hyperthermia.

1.2.1. Whole-body hyperthermia

Whole-body hyperthermia (WBH) is a systemic hyperthermia treatment during which the core temperature of the body is elevated to 39-42°C by heating up the whole body of the patient within thermal chambers, hot water blankets or infrared radiators [25]. This type of hyperthermia can be used for patients of disseminated and metastatic tumors [25,30]. Among the different types of hyperthermia, whole-body hyperthermia is the most

challenging with the highest probability of side effects and complications, thus prudent preselection of the patients is inevitable (e.g. patients with heart, liver, kidney, bone marrow or pulmonary insufficiency should be excluded) [30]. Heating up the body core temperature to 39-42°C is a high burden for the patients, thus treatments are conducted under general anesthesia with strict control of physiological parameters (blood pressure, pulse rate, pO_2/pCO_2, ECG) and electrolyte fluid restoration [25,30]. While local and regional hyperthermic treatments cause only moderate side effects, such as irritation or mild burning of the skin and subcutaneous fat, whole-body hyperthermia can induce among others diarrhea, nausea, vomiting and thermal stress to several organs (most commonly brain, heart, lung and liver) [25,30].

1.2.2. Regional hyperthermia

Regional hyperthermia refers to the hyperthermic treatment of a more extented part of the body, such as the pelvis, the abdominal cavity or the limbs. This type of hyperthermia can be used for treating deep-seated or locally advanced tumors (e.g. cervical and ovarian cancers, rectal cancers, bladder cancers, prostate cancers, soft tissue sarcomas, mesotheliomas and peritoneal carcinomatosis) [25]. The three main methods that can be used for conducting regional hyperthermia are (i) external applicators operating with microwaves, radiofrequency or ultrasound, (ii) thermal perfusion of a limb or one or more organs and (iii) continuous hyperthermic peritoneal perfusion (CHPP) [25]. Another special regional hyperthermic treatment modality for advanced or disseminated malignancies located in the abdominal cavity is hyperthermic intraperitoneal chemotherapy (HIPEC), when the warm perfusion fluid is supplemented with one or more chemotherapeutic agents for improving the treatment efficacy [25].

1.2.3. Local hyperthermia

Local hyperthermia is usually used on superficial (e.g. head and neck cancer, soft tissue sarcomas, breast cancers), intracavital (e.g. tumors in the abdomen, pelvis or chest), intraluminal (e.g. oesophageal cancer, rectal cancer) or intracranial (e.g. gliomas) tumors, which are not bigger than 6 cm in the longest diameter [25]. Local heating techniques use most commonly radiofrequency (13,56 – 100 MHz [31–36]), microwaves (300-2450 MHz [37–45]; most frequently 915 MHz or 2450 MHz are used, as these are allowed for medical, industrial and scientific purpose in the US and worldwide, respectively [39–45]),

or ultrasounds (e.g. High-Intensity Focused Ultrasound, HIFU) to deliver heat to the treated site, but application of hot sources – such as infrared radiators or resistive wire implants – are also used [25]. A fairly new local hyperthermia approach is the use of ferromagnetic nanoparticles for the thermal treatments, which magnetic seeds that are administered intravenously or injected directly to the treatment site are heated up by applying electromagnetic field. This technique allows very precise heat targeting and it is highly suitable for local treatment of deeply seated tumors in the pelvis (prostate cancers, cervical cancers) or in the skull (glioblastomas) [46,47]. A special type of local hyperthermia is thermoablation. During thermoablation the tumorous tissue is heated up over 50°C for 4-6 minutes by laser or radiofrequency applicators [25,48]. At this temperature vascular stasis, coagulation and necrosis occur, which lead to tumor destruction. This method can be used for eradication of very small, focal tumors [25,48].

1.3. Modulated electro-hyperthermia

Modulated electro-hyperthermia (mEHT; trade name: Oncothermia®) is a special type of loco-regional hyperthermia applying capacitive radiofrequency at 13.56 MHz [24]. The communicated energy can be detected as a local temperature rise in the tumor. The mEHT treatment device (EHY-2030 Oncotherm®) consists of two electrodes. The adjustable upper electrode with shape-adapting, water-cooled bolus, fixed on a moveable arm, which can be placed on the treated area of the body. The built-in lower electrode is located in the treatment bed with water mattress, where the patient lies during the treatment (Figure 2.). Since the human body is an excellent conductor, when the upper and the lower electrodes are placed on the treated body region, the patient will be a part of the electric circuit and electromagnetic waves will flow through the treated region during the treatment [24].

Figure 2. The clinically used modulated electro-hyperthermia treatment device EHY-2030 (A) Adjustable upper electrode with shape-adapting, water-cooled bolus, fixed on a moveable arm; (B) Treatment bed with water mattress and built-in lower electrode; (C) Control panel and treatment monitoring [49].

1.3.1. Principles of modulated electro-hyperthermia

Modulated electro-hyperthermia can induce highly selective heating of tumors by capacitive-coupled energy transfer, where the capacitor is the tumor itself [24]. The mechanism of this selective heating is based on the altered complex electric properties of the tumors compared to normal tissues [24]. Conductivity (σ) is the measure of the ease at which an electric charge or heat can pass through a material. Dielectric permittivity (ε) is a diagnostic physical property which characterizes the degree of electrical polarization a material experiences under the influence of an external electric field. Impedance (Z) is a measure of the overall opposition of a circuit to current, in other words: how much the circuit impedes the flow of charge. It is like resistance, but it also considers the effects of capacitance and inductance. The σ and ε values of a malignant tissue are significantly higher than those of the normal tissues around the tumor, which leads to decreased complex impedance of the tumorous tissue [50,51] and, consequently, accumulation of the electromagnetic waves in the tumor, when the patient is treated using radiofrequency (RF) radiation [24]. The energy transferred by radiofrequency current is absorbed dominantly and induces local temperature rise in the tumor, because of the significantly higher local RF-current density [24]. The thermal effect of the RF-current is based on the

dielectric heating phenomenon: the rotation of the dipolar molecules due to the rapid changing of current direction (at 13.56 MHz carrier frequency, the direction of the current changes 13.56 million times/second) generates heat in the dielectric material [24,52].

The background of the decreased impedance of the tumor tissue is quite complex. Since tumors use dominantly anaerobic metabolism to provide ATP (Warburg effect: glucose uptake and preferential production of lactate, even in the presence of oxygen), the final product of this fermentative process – the lactic acid – is highly accumulated, resulting in a lower pH compared to the surrounding normal tissues [53,54], which is an impedance-reducing factor [24]. Furthermore, tumor cells metabolize much faster, than normal cells, requiring a much higher transport activity, consequently a definitive change occurs in the electrolyte composition and concentration of the microenvironment [55]. The higher ionic concentration also lowers the impedance. The higher metabolic rate results in a higher local temperature in the tumor [56], which is another factor contributing to the lower impedance of the tissue [57]. The intracellular and extracellular water levels in the tumor are usually elevated. The water molecules are more disordered, which promote the mobility of the ions and thereby decreases the impedance [58,59]. Besides, in advanced malignancies, when tumor-angiogenesis is active, blood perfusion becomes much higher in the tumor because of its newly developed, rich vasculature, which lowers the impedance of the tissue even more [24,60]. In summary, factors lowering tumor tissue impedance are: lactate acidosis, faster metabolism/transport with higher ion-concentration and temperature, higher water content and hyperperfusion.

Modulated electro-hyperthermia operates with a 13.56 MHz RF-current, which is a constant carrier frequency combined occasionally with fractal amplitude modulation [24]. The 13.56 MHz frequency was chosen because it is a free frequency range, which has no interference with other electrical devices (shielding is not required) and it can penetrate well into the human body (< 25 MHz) [24]. Furthermore, it is safe, since it is far above the level of neural excitation (around 10 kHz) and below microwave radiation (around 1 GHz) [24]. The frequency around 10 MHz has a favorable effect on the cellular membrane and is also optimal for low frequency modulation (up to 20 kHz) [24].

1.3.2. Biological impacts of modulated electro-hyperthermia

Modulated electro-hyperthermia has several thermal and non-thermal effects. Thermal effects are direct consequences of the elevated temperature and they are absolutely temperature-dependent. At macroscopic level, hyperthermia causes robust vascular and blood flow changes [61,62], which are highly distinct between tumorous and normal tissues [63]. It has been described that at elevated temperatures tumor blood vessels contract and perfusion becomes significantly lower compared to the surrounding healthy tissues, where concomitantly vasodilatation occurs [24,63]. Decreased blood flow leads to hypoxia, while also functions as a heat trap in the tumor (cooling effect of the blood perfusion cannot prevail) [24,64]. At the cellular level, mild hyperthermia – under 39°C – increases biochemical reaction rates, cell metabolism and cell growth [24,26]. Above 39°C may blockade the mitotic cycle (39-40°C) takes place, and irreversible cellular damage and cell death occur over 40°C. These effects may result from the heat-inhibited DNA replication [65,66] and from the cell membrane changes, e.g. softening of the lipid bilayer, changes in lipid-protein interactions and protein denaturation [24]. These mechanisms also affect the transport proteins, resulting in altered ion gradient (K^+, Na^+ and Ca^{2+}), membrane potential and cellular function [67]. Electrically excitable cells can be blocked by thermal treatment [68]. During hyperthermia the initially induced cell metabolism leads to enhanced glycolysis and production of lactic acid, which rapidly lowers the pH of the tissue and provokes cell stress [24,53]. Furthermore, at low pH (pH $\approx$ 6) and elevated temperature (41°C) complete blockade of tumor blood perfusion can occur [26,69], worsening even more the hypoxia of the cells. The initially elevated cell metabolism uses up all cellular ATP. ATP depletion leads to electrolyte imbalance, protein aggregation, cytoskeletal and plasma membrane damage and finally cell death [24].

Non-thermal effects of modulated electro-hyperthermia are mediated by the alternating electromagnetic field. The non-thermal effects are mainly frequency-dependent and result from the interaction of the biological substance with the RF-current [26]. These effects can be classified into four groups: (i) polarization effects, (ii) membranotropic effects, (iii) molecular effects and (iv) macro effects [70]. Polarization effects of the RF-current-generated electromagnetic field (EMF) are the electrophoresis of dielectric particles [71] and the orientation and rotation of cells and cell nuclei [72].

EMF-induced membranotropic effects are electroporation and electro-permeabilization, which lead to changes in cell membrane structure and function (e.g. transmembrane transport) and can even result in fusion of the cells [73,74]. Molecular effects refer to the altering expression and functions induced by EMF on macromolecules, including DNA and proteins. The exact basis of the interaction between these macromolecules and EMF are still not clarified, but some papers suggest that EMF may interfere with these macromolecules, which can absorb the energy of the RF-current (at low frequencies) [75]. The absorbed energy can catalyze biochemical reactions (e.g. enzyme functions) [76] and influence the transcriptional features of the DNA (e.g. induced transcription of certain mRNAs, such as those of heat shock proteins (Hsps)) [77,78]. Finally, EMF also has macro effects, which are cumulated from the micro effects, discussed above. As a summation of polarization, membranotropic effects and interference with biologically active macromolecules, during modulated electro-hyperthermia the RF-current-generated alternating electromagnetic field diminishes cell proliferation [79], causes mitotic catastrophe [80] and induces cell death [81,82].

1.4 Heat shock response

Heat shock response (HSR) of living organisms is an ancient and universal mechanism, which refers to a complex molecular defense process activated upon cell stress [83]. Although the first observations of this mechanism were made upon heat shock [84,85], it is already known that not only heat, but several other cell stress-inducing factors such as oxidative stress, heavy metals and other toxic agents can provoke the heat shock response, which is intended to protect the cell from damage [86–88].

Heat shock – or more generally cell stress – induces disturbance in protein homeostasis, cytoskeletal structure, nuclear processes and brings about changes in the cell membranes [83]. Since proteins are very sensitive to any kind of changes of the microenvironment, heat or other stress factors heavily affect their structure and function [83]. Upon cell stress foremost protein misfolding and unfolding occur, which lead to nonfunctional proteins, moreover entanglement and aggregation of the protein molecules [89,90]. The dysfunction cytoskeletal proteins can disrupt the intracellular localization of the cell organelles and interfere with intracellular transport [91]. Upon serious heat shock, the endoplasmic reticulum, Golgi network, mitochondria and lysosomes can get

fragmented [90] and mitochondrial damage could eventually lead to the abrogation of oxidative phosphorylation and ATP production [92]. Nuclear processes can also get damaged leading to deregulated RNA splicing [93,94], aggregation of RNA chains and eventually a global decrease in translational activity [90,95,96]. Morphology of the cell membrane and intracellular membranes also get altered upon robust cell stress, resulting in increased fluidity and permeability and, consequently, changes in the pH and ion homeostasis [83,97]. All of these effects together result in the stagnation of cell growth and proliferation through cell cycle arrest and finally death of the cells [83,94,98].

The morphological and functional changes discussed above trigger the heat shock response, which strictly speaking is a rapid and transient gene transcription program in order to protect the organism against damage [83]. The main effectors of the heat shock response are the so-called heat shock proteins, like Hsp70 and Hsp90, which are molecular chaperons and, as such, they are able to recognize and refold or assist in eliminating misfolded proteins [83,99–101]. When cell stress occurs, misfolded proteins induces the transcription of Hsps, which restore normal protein homeostasis [83]. The transcription of Hsps is initiated by the transcription factor heat shock factor-1 (Hsf-1) [83,102]. Under physiological conditions Hsf-1 monomers are located in the cytosol and they form complexes with Hsp molecules (mainly Hsp70 and Hsp90) [83,102]. Upon cell stress Hsps recognize the hydrophobic polypeptide chains of the misfolded proteins and dissociate from the Hsf-1/Hsp complex to repair the nonfunctional proteins [83,102]. Free Hsf-1 monomers form homotrimers in the cytosol, which is a sign for nuclear translocation [83,102]. Nuclear Hsf-1 trimers get hyperphosphorylated, bind to the heat shock element (HSE) on the DNA and induce the transcription of Hsps [83,102].

1.4.1. Inhibitors of the heat shock response

Activation of the heat shock response provides protection for the tumor cells against the heat-, radiation- or chemotherapy-induced damage, and thus it attenuates the efficiency of antitumor treatments [99,101]. It has been already described that overexpression of the heat shock proteins is one of the survival mechanisms of cancers, which helps them to resist therapies [101]. Inhibition of this defense mechanism could sensitize the tumor cells to hyperthermia or other antitumor therapies.

1.4.1.1. Quercetin

Quercetin (3,3',4',5,7-pentahydroxyflavone) is a well-known phyto-flavonoid present in several plants, and therefore a common compound of the normal human diet [103–105]. Its biological impacts such as its anti-inflammatory, antioxidant and anti-cancer effects have already been widely explored *in vitro* and *in vivo* [104–106]. A special feature of this compound is the ability of inhibiting the heat shock response by diminishing the activity of Hsf-1 [107,108]. Quercetin is able to block Hsf-1 kinases and thus the activation (hyperphosphorylation) of Hsf-1 [107–109]. In the absence of hyperphosphorylation, Hsf-1 cannot bind to the heat shock element on the DNA, preventing transcription of Hsps [107,108,110]. However, quercetin is a potent HSR inhibitor, which also affects apoptotic pathways, cell cycle, metastatic processes, autophagy and angiogenesis, ergo it has pleiotropic ways of action [104,111].

1.4.1.2. KRIBB11

KRIBB11 (N2-(1H-indazole-5-yl)-N6-methyl-3-nitropyridine-2,6-diamine) is a novel synthetic low-molecular-weight inhibitor of the heat shock response, which has been introduced by Yoon et al. in 2011. This molecule is the first direct inhibitor of Hsf-1, since it binds straight to Hsf-1 and blocks its Hsp-inducing activity [112]. KRIBB11 is a highly selective and potent inhibitor of HSR both *in vitro* and *in vivo* [112–114].

2. Objectives

The studies summarized in this thesis are aimed to investigate the macro- and micromolecular effects of mEHT in the 4T1 triple-negative breast cancer models both *in vitro* and *in vivo* by focusing on:

- the development of a rodent modulated electro-hyperthermia device for orthotopic mouse breast cancer treatment *in vivo*
- the tumor cell killing and tumor destructive effects of repeated mEHT *in vivo*
- the apoptosis-inducing effects of repeated mEHT *in vivo*
- the temporal changes in mEHT effectiveness *in vivo*
- the heat shock response and its dynamics after repeated mEHT treatments *in vivo*
- the synergistic effects of mEHT and heat shock response inhibitors (quercetin and KRIBB11) *in vitro*

3. Results

All experiments presented below have been approved by the National Scientific Ethical Committee on Animal Experimentation under permission numbers PE/EA/633-5/2018 and PE/EA/50-2/2019.

3.1. Development of a more feasible and accurate *in vivo* treatment setup

Until 2020 the standard preclinical mEHT treatment setup for treating small animals was the LabEHY-100 device with a tissue electrode provided by the Oncotherm® company (Figure 3. A). However, this setup was not optimal for treating tumors in the inguinal region of mice, since the tissue electrode was too large (total area: 1385 mm^2, conductive area: 490 mm^2), so it did not adapt properly to the concave surface, therefore skin contact and coupling were inappropriate (Figure 3. A). As a consequence, mEHT also elevated the rectal temperature (representing the core temperature of the animal) during treatment (Figure 3. C). Thus, treatment implementations were problematic, temperature curves were highly variable, more power had to be applied and treatments caused heat-related side effects such as skin burning.

The development of the LabEHY-200 device with pole electrode in cooperation with the engineers of Oncotherm® resulted in an improved small animal treating setup which was optimized for treating the mammary tumors of mice. Technical improvements of the LabEHY device included a new tuning method performed by a warbler which is identical to the clinically used method. The new device is connected to a PC through a USB port and the treatment parameters (time, power, modulation) can be adjusted by the software with a more user-friendly graphical interface. The new ergonomic pole electrode adapts to the surface of the tumor and the inguinal region, and the size of the electrode was optimized (conductive area: 255 mm2; Figure 3. B).

With the LabEHY-200 and the newly developed pole electrode a more accurate skin-electrode contact was achieved, thus tissue coupling improved. The treatments became more efficient and standard even at lower power (Figure 3. D), and the more focused treatments prevented heat-related side effects. Better focus and coupling reduced the variability in temperature and power during treatments. The rectal temperature remained within the normal range (T_{rectal} = 37.03 ± 0.61 °C) and treatments became local and reproducible (Figure 4.).

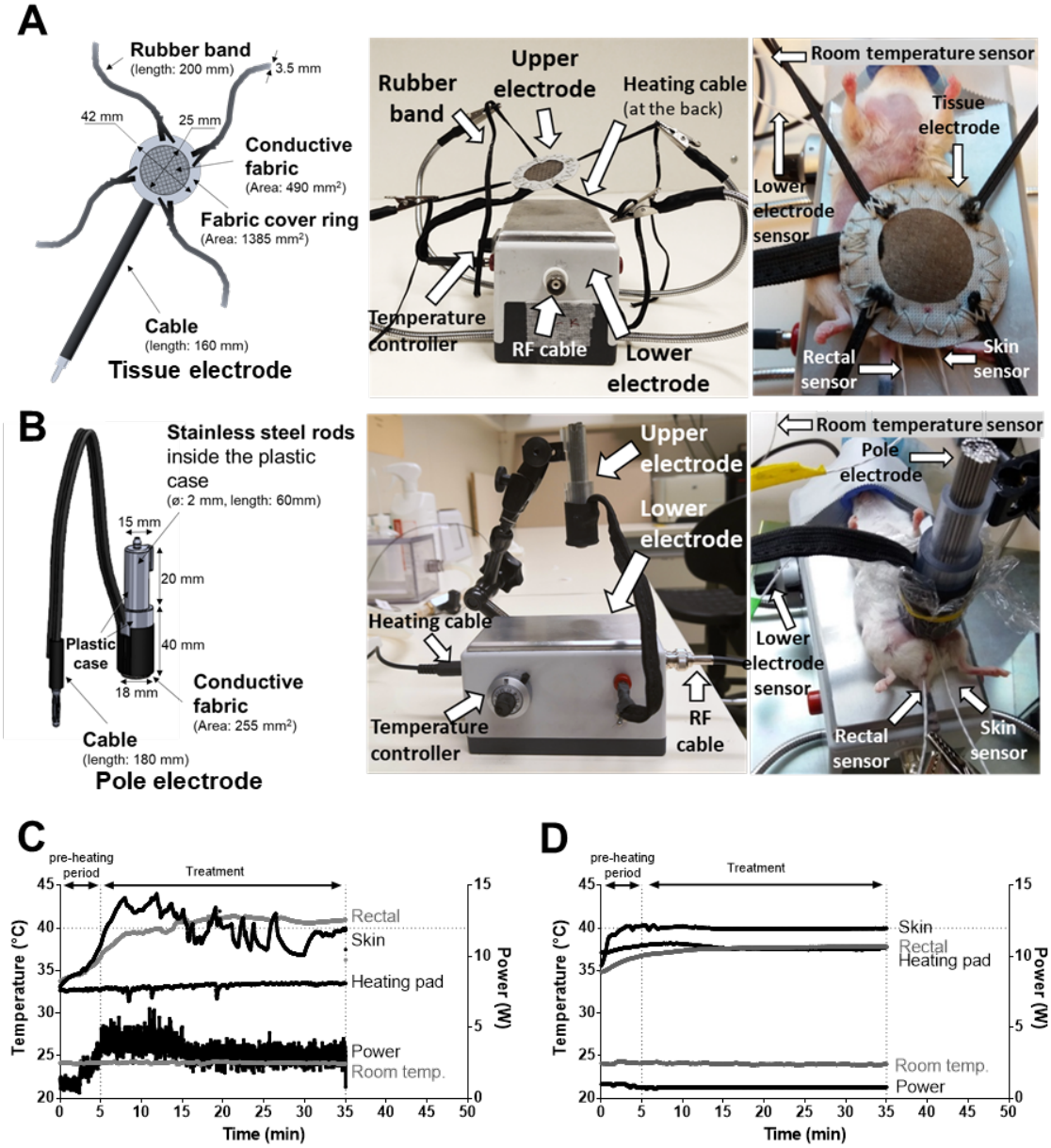

Figure 3. Comparison of LabEHY-100 with tissue electrode and LabEHY-200 with pole electrode (**A**) Tissue electrode and treatment setup (**B**) Improved ergonomic pole electrode and treatment setup (**C**) Representative recording of skin, rectal, heating pad and room temperatures and applied power during a treatment with LabEHY-100 and tissue electrode; (**D**) Representative recording of skin, rectal, heating pad and room temperatures and applied power during a treatment with LabEHY-200 and pole electrode [18].

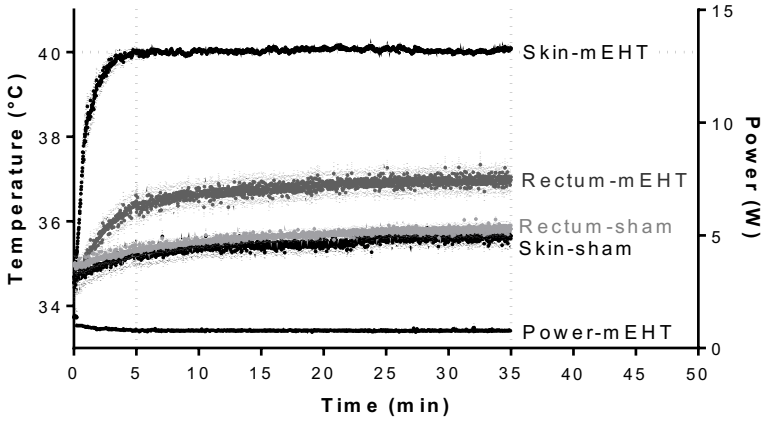

Figure 4. Temperature recordings of mEHT treatments with LabEHY-200 and pole electrode Skin and rectal temperature and applied power recordings from 12 mEHT and 12 sham treatments with LabEHY-200 and pole electrode. *n* = 12/group, Mean ± SEM [18].

3.2. mEHT induced local temperature rise in the tumor

The mEHT treatments were performed in a temperature-driven way, that is, the applied power was adjusted to heat up the tumor to 42°C. To properly adjust the amount of energy delivered into the tumor by mEHT, we determined the temperature within the tumor and its surroundings (skin, rectum) in a pilot experiment (Figure 5.). Temperatures were monitored by a four-channel TM200 thermometer, the four temperature sensors were positioned (i) directly into the core of the tumor, (ii) on the skin above the tumor, (iii) in the rectum and (iv) on the surface of the heating pad (Figure 5. A). The tumor temperature was 2.5 ± 0.5°C higher ($p < 0.0001$) compared to the skin directly above the tumor (Figure 5. B, C) and 4.4 ± 1.2 °C higher ($p < 0.0001$) than in the rectum below the tumor (Figure 5. D). Based on these findings, only the noninvasive rectal and skin temperatures were recorded in all further experiments to monitor the energy communicated to the tumor without any mechanical injury of the tumor.

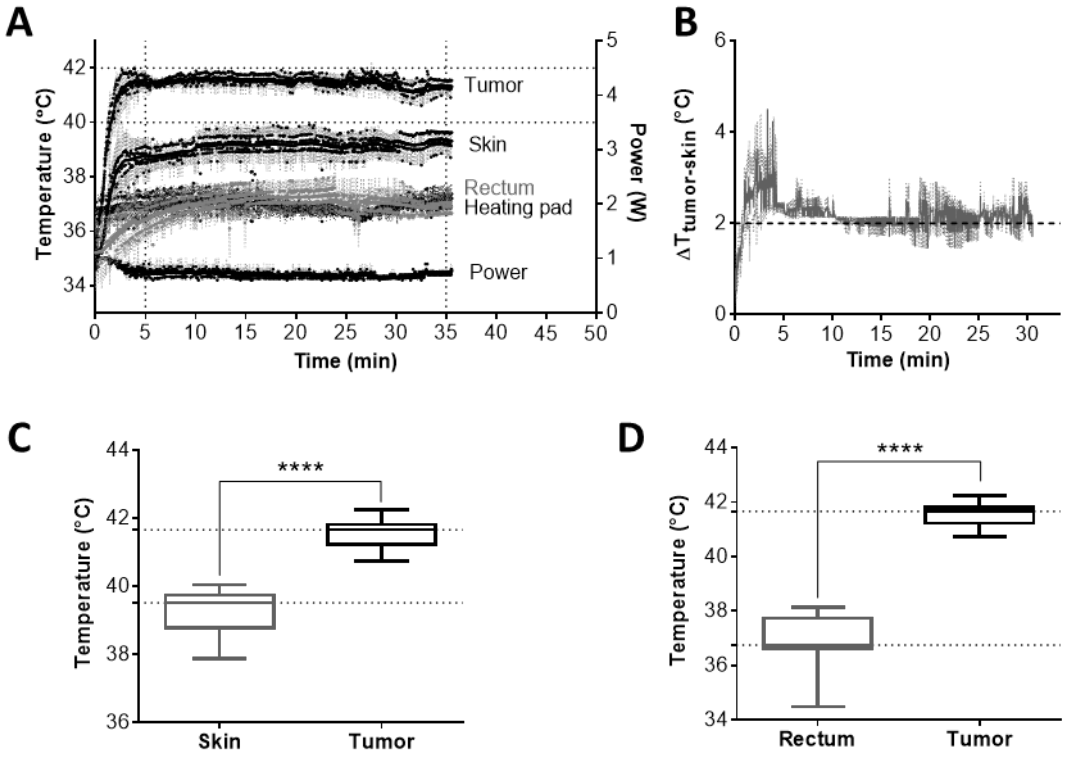

Figure 5. Selective warming of the tumor tissue (**A**) Temperature curves of the tumor, skin, and rectum during mEHT-treatment; (**B**) Temperature gradient between the tumor core and skin above the tumor; (**C**, **D**) Temperature of skin (**C**) or rectum (**D**) vs. tumor core during treatment; n=5, (**A, B**) Mean ± SEM; (**C, D**) Average and box and whiskers: min to max, **** $p < 0.0001$ [18].

3.3. mEHT decreased the number of viable tumor cells but did not influence tumor size after only two treatments

For investigating the prompt cell-killing effect of mEHT *in vivo*, we inoculated firefly luciferase transfected 4T1 cells ortotopically into mice using 1:1 Matrigel®-PBS matrix as vehiculum for augmented tumor growth and better tumor integrity. Then we monitored the amount of viable cells after mEHT treatments by the IVIS In Vivo Imaging System. In the presence of D-luciferin the viable 4T1 cells, which stably express the luciferase enzyme, cleave luciferin, which is accompanied by fluorescent light emission. The requirement of cellular ATP means that only viable tumor cells emit light. Thus, there is a quantitative correlation between the intensity of the emitted light and the number of viable tumor cells. The measurements were performed 24 hours before and after the mEHT treatments. Luciferin was dissolved in 0.9% NaCl solution and was administered via intraperitoneal injection to the mice 10 minutes before the measurement. We could demonstrate that luciferase-transfected viable 4T1 cells emitting fluorescent light were

significantly reduced already after two consecutive mEHT treatments ($p = 0.0082$; Figure 6. A, B).

We also measured the tumor volume with more conventional techniques using digital caliper and ultrasound. Two mEHT treatments did not reduce significantly tumor sizes as measured by these methods (Figure 6. C, D). Neither was the tumor weight reduced at termination 24 h after the second mEHT treatment (Figure 6. E).

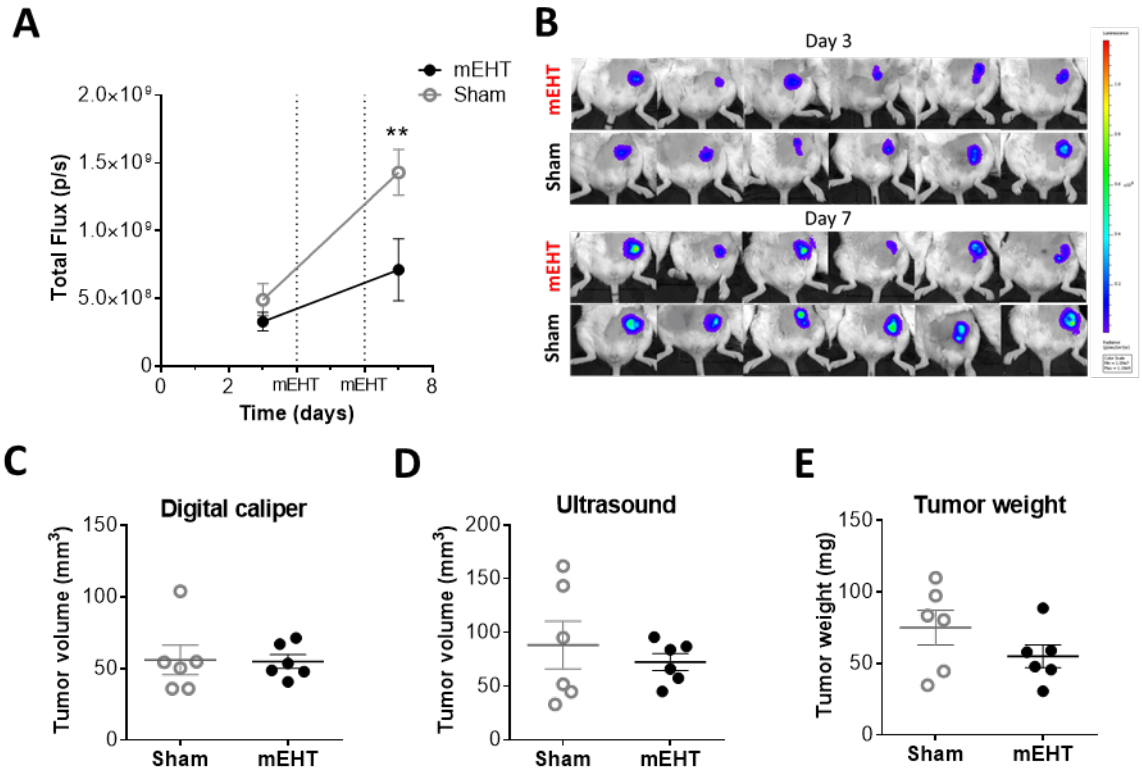

Figure 6. The effects of modulated electro-hyperthermia (mEHT) on tumor size (**A**,**B**) Total fluorescent flux measured by IVIS 24 h before and after two mEHT treatments; (**C**, **D**) Tumor volumes after two mEHT treatments, measured by (**C**) digital caliper and (**D**) ultrasound (**E**) Tumor weight after resection (24h post-treatment); Mean ± SEM; $n = 6$/group; (**A**) two-way ANOVA, Bonferroni correction, ** $p < 0.01$; (**C**–**E**) Mann–Whitney test [18].

3.4. Two mEHT treatment induced tumor destruction

The reduced number of vital tumor cells—as detected by IVIS—was strongly corroborated by the histologic analysis of the tumors. The damage of the tumorous tissue was quantified on histological sections from the resected tumors by the Tumor Destruction Ratio (TDR), which was defined as the ratio of the whole tumor area and the damaged tumor area. On hematoxylin and eosin (H&E) stained sections tissue damage appeared as pale, eosinophilic areas due to vacuolized cytoplasm and shrunk or

fragmented nuclei of damaged tumor cells, which could be clearly differentiated from the morphologically undamaged cells and also from the unstructured, homogenous, cell-poor eosinophilic Matrigel residues (Figure 7. A-C).

Following two mEHT treatments, TDR was significantly higher in the mEHT-treated tumors than in the sham-treated ones based on the analysis of the H&E-stained sections (p = 0.0174; Figure 7. D).

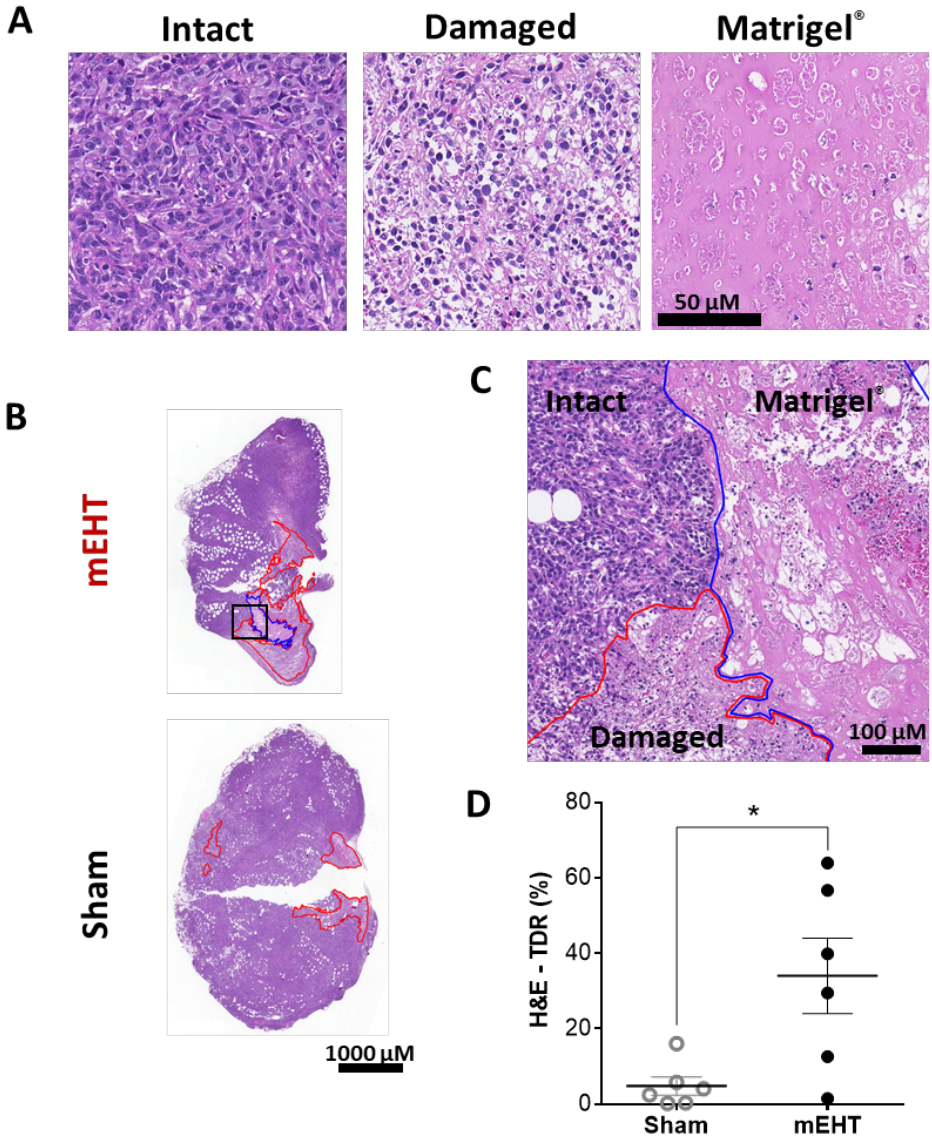

Figure 7. mEHT induced tumor destruction 24h after two treatments (**A**) Matrigel®, damaged and intact tumor areas on H&E-stained sections (Magnification: 36×); (**B**) Apoptotic areas (red contour) and Matrigel® (blue contour) on representative H&E-stained sections; (**C**) Representative image of intact vs. damaged area and Matrigel® (magnified from the H&E section (**B**) black rectangle, magnification: 8.5×); (**D**) Tumor destruction ratio (TDR) evaluated on hematoxylin-eosin (H&E) stained sections; Mean ± SEM, Mann–Whitney test, n = 6/group, * $p < 0.05$ [18].

3.5. Two mEHT-treatments induced caspase-dependent apoptosis

To identify the way of cell death provoked by mEHT, we analyzed cleaved caspase-3 (cC3) immunohistochemical staining of the histological sections from resected tumors. Cleaved caspase-3 – the activated form of caspase-3 – is a widely used marker of programmed cell death, as it plays a central role in the caspase-cascade mediated apoptosis [115].

Analysis of the cC3-immunostained sections showed that the cC3-positive, apoptotic areas extensively overlapped with the damaged areas seen on consecutive H&E sections, which confirmed that the mEHT-related tissue damage was a consequence of the treatment-induced programmed death of the tumor cells (Figure 8. A-C). In addition, a significant increase (**p=0.0020) in the cC3-positive areas could be detected in the tumors after two mEHT treatments compared to the sham-treated tumors (Figure 8. D), which demonstrated that mEHT treatment induced apoptotic cell death in the tumor.

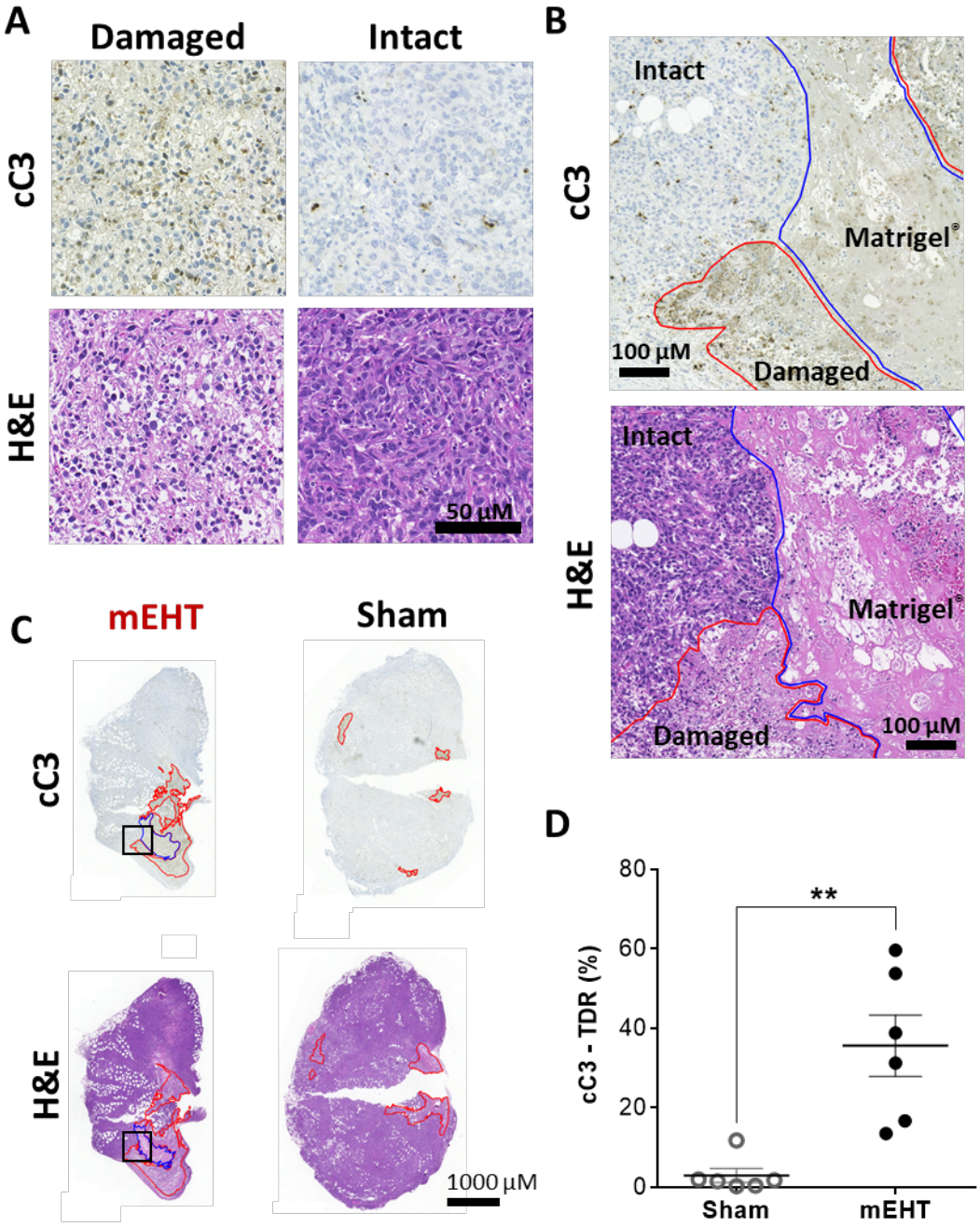

Figure 8. mEHT-induced tumor destruction was mediated by cleaved caspase-3 (cC3) (**A**) Damaged and intact tumor areas on cC3- and H&E-stained sections (Magnification: 36×); (**B**) Representative images of intact vs. damaged area and Matrigel® (magnified from H&E and cC3 sections (C) black rectangles, magnification: 8.5×); (**C**) Apoptotic areas (red contour) and Matrigel® (blue contour) on representative cC3-stained sections and consecutive H&E-stained sections. (**D**) Tissue destruction ratio (TDR) evaluated in cC3-stained sections; Mean ± SEM, Mann–Whitney test, $n = 6$/group, ** $p < 0.01$ [18].

3.6. Repeated mEHT induced hypocellularity on a short-term and reduced the Ki67 expression of treated tumors on a long-term

For investigating the short-term and long-term effects of repeated mEHT treatments on the proliferation activity of the cells, we examined the cell density of the tumors by immunostaining cell nuclei using Ki67-specific antibodies revealed with 3,3'-diaminobenzidine (DAB, brown) chromogen following two or five mEHT treatments.

The total number of cell nuclei in the viable part of the tumors – evaluated on Ki67/DAB-stained sections – was significantly smaller in the mEHT-treated tumors compared to the sham-treated tumors after two treatments, resulting in a lower density of viable tumor cells in the mEHT-treated tumors (Figure 9. A, B).

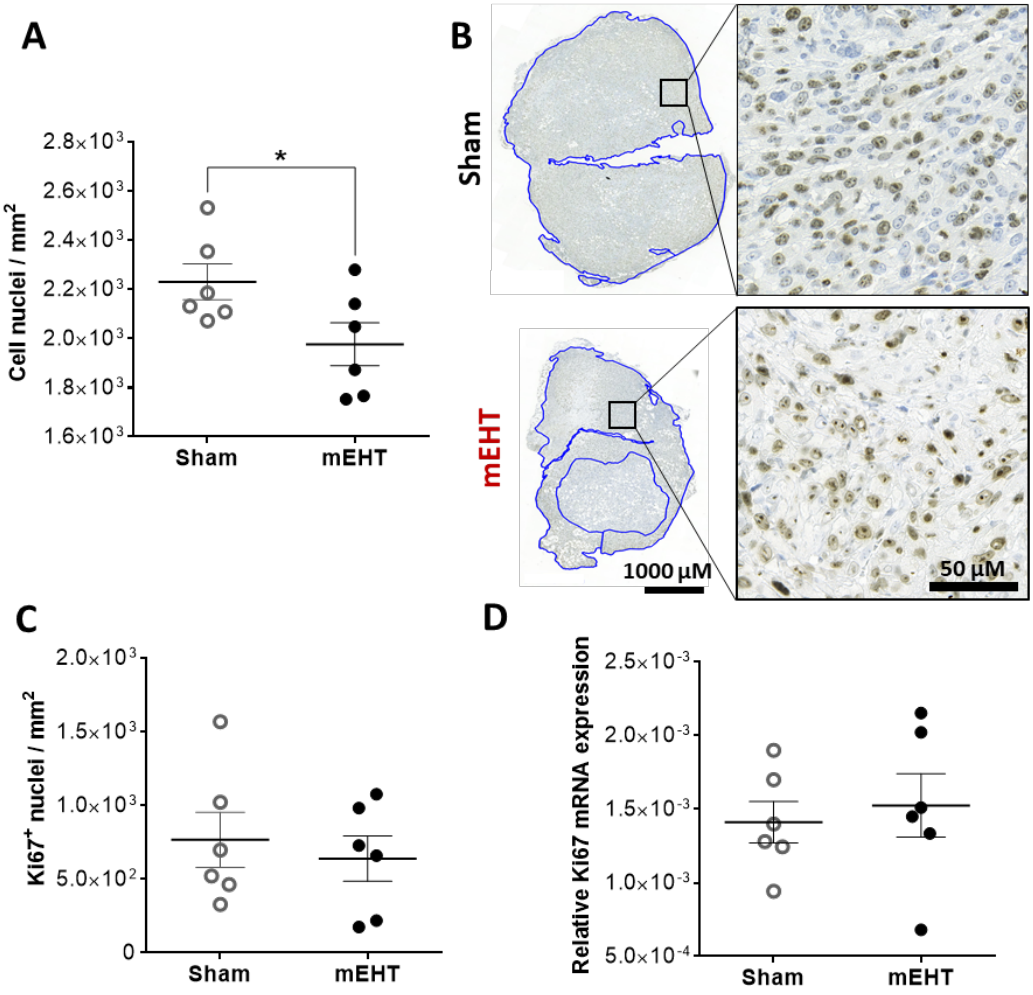

Figure 9. Ki67 expression 24 h after two mEHT treatments (**A**) Number of cell nuclei/mm^2 in the intact tumor areas; (**B**) Ki67 staining in the viable tumor tissue (blue assigned areas), representative sections; (**C**) Number of strong Ki67-positive nuclei/mm^2 in the intact tumor areas; (**D**) Ki67 mRNA expression in tumor tissue from half tumor homogenate (normalized to 18 S rRNA); Mean ± SEM, unpaired t-test, n=6/group, *p < 0.05 [18].

This finding strongly supported the observation of less viable tumor cells with IVIS after two mEHT treatments. The number of Ki67-positive nuclei evaluated in the intact tumor area (Figure 9. C) as well as Ki67 mRNA (Figure 9. D) was similar between the groups, suggesting that mEHT treatments on a short-term did not affect strongly the proliferation activity of the tumor cells.

We analyzed the same parameters – cell density and Ki67 expression – from a separate experiment, where 4T07 isografts were treated five times with mEHT following the same protocol as before. In our experiments these isografts has a very similar nature and growth rate in Balb/C mice as 4T1 isografts. The sections showed a clearly visible difference between the sham- and mEHT-treated groups after five treatments, as all sham-treated tumors were dark brown but all mEHT tumors were pale (Figure 10. A). At higher magnification we could see that sham-treated tumors were extremely dense – based on DAB staining of the cell nuclei – and strongly positive for Ki67, whereas mEHT-treated tumors appeared to be much less dense (Figure 10. B) and less Ki67-positive nuclei could be detected (Figure 10. C).

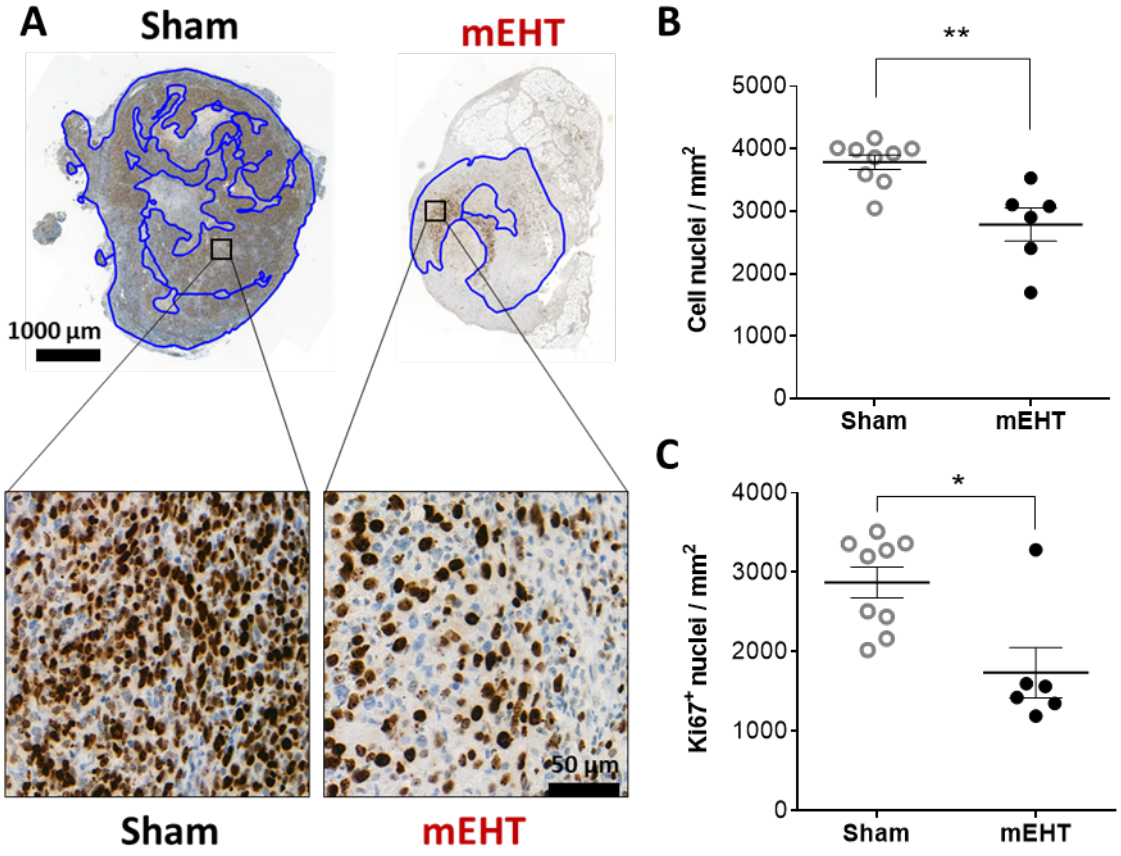

Figure 10. Ki67 expression 24h after five mEHT treatments (**A**) Ki67 staining in the viable tumor tissue (blue assigned areas), representative sections; (**B**) Number of cell nuclei/mm^2 in the intact tumor areas; (**C**) Number of strong Ki67-positive nuclei/mm^2 in the intact tumor areas; Mean ± SEM, unpaired t-test, n = 6-9/group, *p < 0.05, **p < 0.01 [23].

Quantification of the cell nuclei/mm^2 parameter in the viable tumor area after five treatments showed a significant decrease in the case of mEHT-treated tumors compared to sham-treated ones, similarly as after two treatments (Figure 9. A; Figure 10. B). However, there was a significant reduction in the Ki67 expression of the tumors after five mEHT treatments compared to sham treatments, which could not be seen after only two mEHT treatments (Figure 9. C; Figure 10. C). With the five mEHT treatments protocol we could demonstrate that mEHT is able to diminish significatnly the proliferation activity of the tumors as a long-term effect.

3.7. Repeated mEHT induced heat shock protein 70 (Hsp70) in viable tumor cells

Hsp70 is one of the most abundant molecules, which gets highly overexpressed upon cell stress (e.g. hyperthermia) in order to activate and mediate defense mechanisms – i. e. heat shock response – to help the organism to survive. Since heat shock response is one of the most important protective mechanisms used by tumor cells to survive treatment-related damage, we intended to investigate whether mEHT treatments provoked Hsp70 expression in our 4T1 isograft model.

Twenty-four hours after two mEHT treatments the tumors had intense Hsp70-specific dark brown (DAB) immunostaining. The staining was especially intense in the viable tumor cells surrounding the damaged tumor areas. Similar intense, specific staining was absent in sham-treated tumors ($p = 0.0028$; Figure 11. A, B), indicating that it was a strong mEHT-related overexpression of Hsp70 at the protein level in the surviving tumor cells. We also examined the Hsp70 expression at mRNA level by real-time qPCR measurements. At the same time point, Hsp70 mRNA was also elevated in some of the mEHT-treated tumors but not in all of them (Figure 11. C), thus mRNA was only tendentially but not significantly higher in the mEHT-treated tumor homogenates twenty-four hours post-treatment.

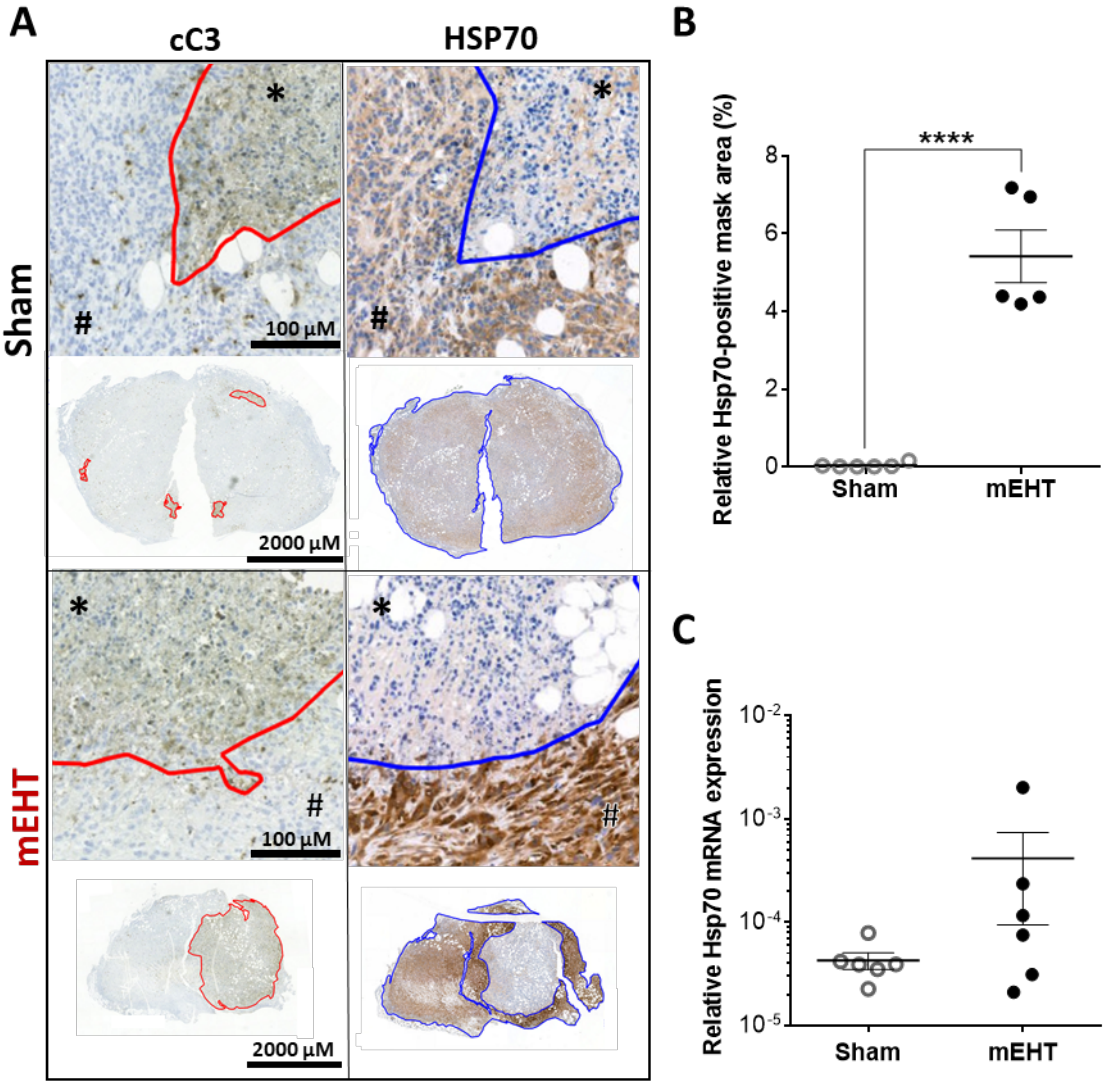

Figure 11. Heat shock protein 70 (Hsp70) expression in tumor tissue 24 h after two mEHT treatments (**A**) Representative cC3- and Hsp70-stained sections with high and low magnification. The damaged area is cC3-positive (marked with *). The living area is cC3-negative (marked with #). Red line: the border of the damaged areas. Hsp70 expression was measured in the living area (marked with #). Blue line: borders of the living areas; (**B**) Relative Hsp70-stained mask area of the viable tumor tissue. (**C**) Hsp70 mRNA expression (normalized to 18S rRNA); Mean ± SEM, Mann-Whitney test, $n = 6$/group, **** $p < 0.0001$ [18].

Since Hsp70 is a very potent protector of the tumor cells against mEHT-induced damage [83], it is crucial to know the dynamics of the overexpression upon treatment in order to be able to optimize therapy. Thus, we performed a time kinetics experiment, where the 4T1 isografts were treated three times with mEHT, followed by sampling of the tumors at 4, 12, 24, 48, and 72 hours after the last mEHT treatment.

This experiment showed that Hsp70 mRNA peaked as early as 4 h post-treatment and started to decline already at 12 h in most tumors (Figure 12. A). At 24 h Hsp70 mRNA was already at the sham level in all, except one tumor, and decreased further in the 48- and 72-h post-treatment groups (Figure 12. A). On immunostained sections, there was a significant elevation of Hsp70 protein already at 4 h post-treatment, but the peak of overexpression was at 12 h post-treatment, closely following the dynamics of the Hsp70 mRNA expression (Figure 12. A, B). Hsp70 protein level started to decrease at 24 h post-treatment compared to the 12 h post-treatment group, but it was still significantly elevated at this timepoint compared to the sham group (Figure 12. B–D). Hsp70 protein levels returned to the sham level in all tumors 48 h post-treatment and remained low at 72 h post-treatment similarly to Hsp70 mRNA (Figure 12.).

Our data show that the Hsp70-mediated protection of the tumors against mEHT therapy is short and temporary, and is exhausted by 48 h after the treatment.

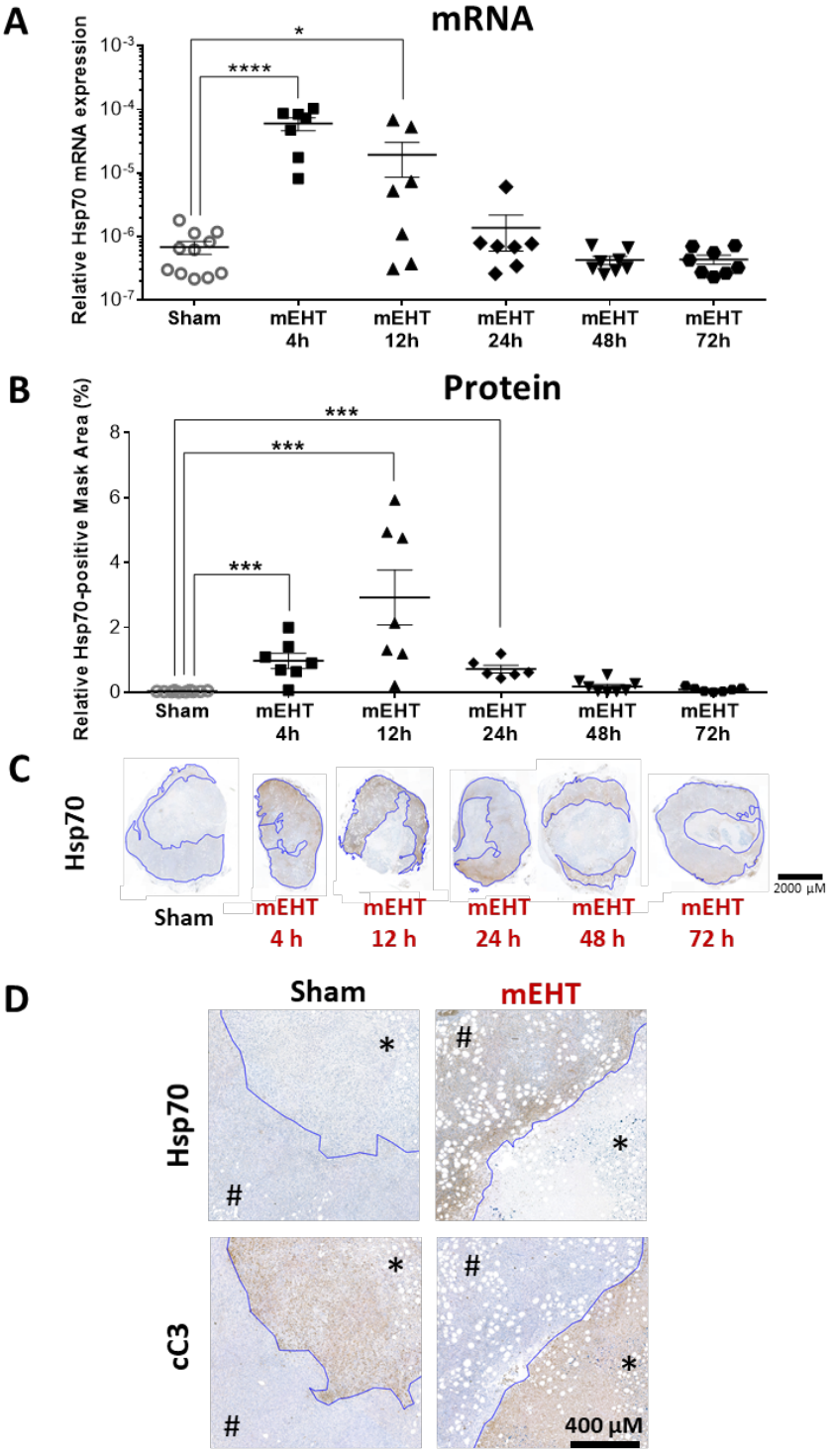

Figure 12. Time kinetics of Hsp70 expression after three mEHT treatments (**A**) Hsp70 mRNA expression of the tumors at different time-points after treatment; (**B**) Area-proportional expression of Hsp70 protein at different time points after treatment; (**C**) Representative tumor images from the sham and mEHT groups; (**D**) High-magnification images of cC3 and Hsp70 immunostainings from sham- and mEHT-treated tumors. Blue line marks the border between live and damaged tumor areas assigned based on the cC3-stainings * marks damaged areas (based on cC3-positivity), # marks viable areas (based on cC3-negativity) (Magnification: 5×); (**A**, **B**) sham vs. mEHT, unpaired Mann–Whitney test. Mean ± SEM, * $p < 0.05$, *** $p < 0.001$, **** $p < 0.0001$. [18]

3.8. Tumor-destructive effect of mEHT was time-dependent

We aimed to investigate the dynamics of mEHT-induced tissue damage and programmed cell death to examine the temporal changes in mEHT effectiveness. For this reason, we evaluated TDR (%) both on H&E- (indicated as H&E-TDR (%)) and on cC3-immunostained sections (indicated as cC3-TDR (%)) at different time points following three consecutive mEHT treatments.

According to our results, H&E-TDR (%) was already significantly elevated 12 h post-treatment, but reached its peak 24 h after the third treatment, compared to sham (Figure 13. A, B). This finding was in good agreement with our previous data, which demonstrated that the protective mechanisms, marked by Hsp70 expression, has already started to decline by this time (Figure 12. A, B; Figure 13. A, B). Our results also demonstrated that the mEHT-induced tumor damage was robust and long lasting, as TDR (%) was still significantly higher 72 h after the treatments compared to sham treatments (Figure 13. A, B).

The proportion of the cC3-positive, apoptotic area compared to the whole tumor area (cC3-TDR (%)) also increased significantly in the mEHT-treated tumors at 12h post-treatment and peaked at 24h post-treatment (Figure 13. C, D). Both the dynamics and the magnitude of elevation highly overlapped with the H&E-TDR (%) changes, just as the location of the cC3-positive areas on the IHC sections with the damaged areas on the consecutive H&E sections (Figure 13.).

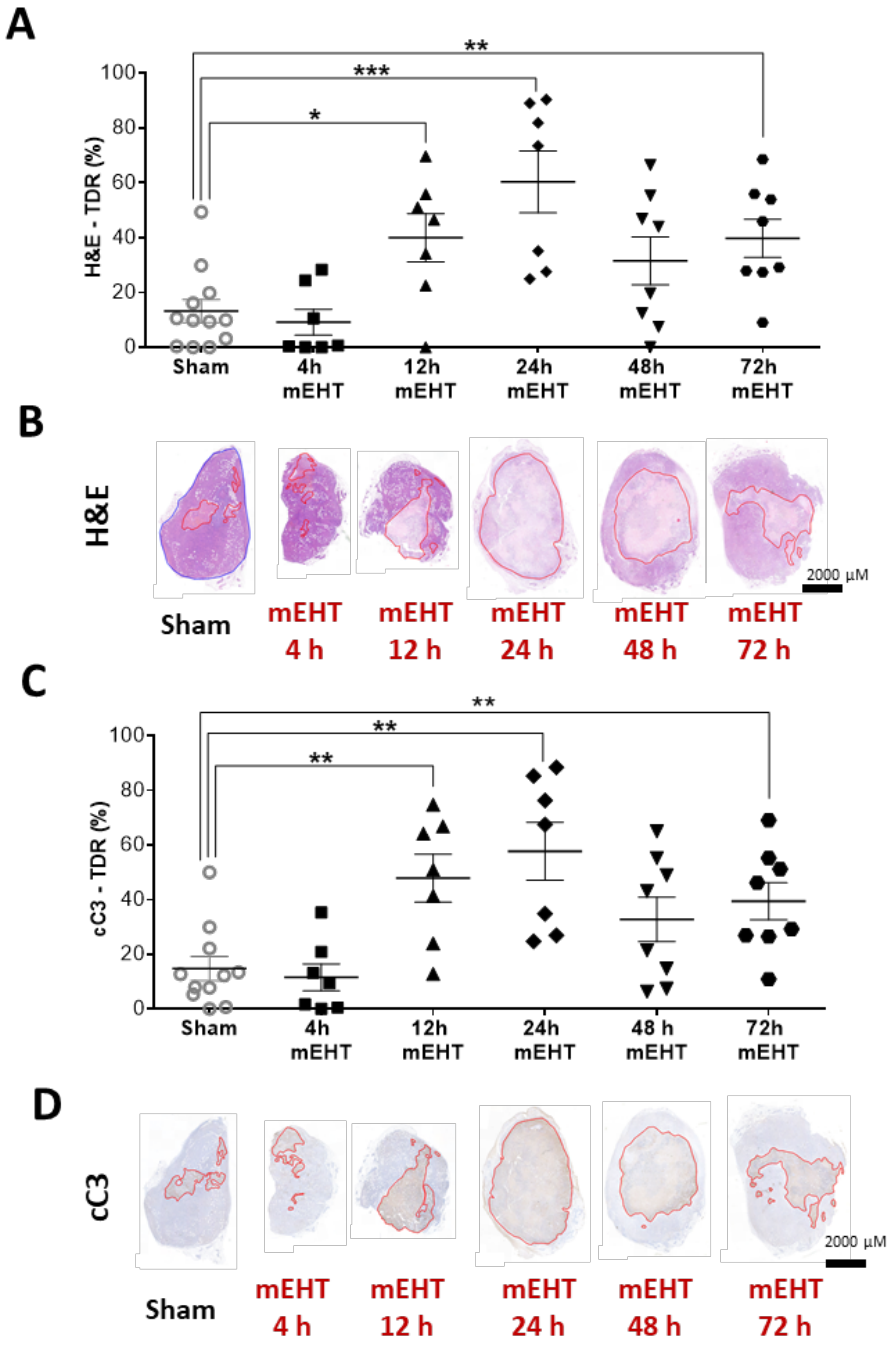

Figure 13. Time kinetics of tumor tissue destruction after mEHT (**A**) Quantification of tumor destruction ratio (TDR %) on hematoxylin-eosin (H&E)-stained sections; (**B**) Representative images of H&E-stained sections from sham and mEHT-treated tumors from 4, 12, 24, 48, and 72 h after 3 treatments. Red lines mark the damaged areas; (**C**) Quantification of TDR % on cleaved caspase-3(cC3)- stained sections from sham- and mEHT-treated tumors; (**D**) Representative images of cC3-stained sections from sham- and mEHT-treated tumors. Red lines mark the damaged areas; **A**, **C**) unpaired Mann–Whitney test. Mean ± SEM, n = 6–12/group, * $p < 0.05$, ** $p < 0.01$, *** $p < 0.001$) [18].

3.9. The tumor-cell-killing effect of mEHT was enhanced synergistically by combination with heat shock inhibitors *in vitro*

We hypothesized that inhibition of the protective heat shock response of the tumor cells by blocking Hsp70 overexpression could improve the treatment outcome of mEHT. To examine this hypothesis, we treated 4T1 cells *in vitro* with two potent heat shock response inhibitors, quercetin and KRIBB11 in combination with mEHT.

First, we demonstrated that *in vitro* mEHT treatment was effective, as Hsp70 mRNA was robustly upregulated 2 hours after the mEHT treatment compared to control (Figure 14. A). In our *in vitro* model both inhibitors were able to diminish significantly the overexpression of Hsp70 mRNA compared to the vehiculum (dimethyl sulfoxide, DMSO) treated control after mEHT treatment (Figure 14. A). The more specific HSR inhibitor KRIBB11 could decrease ($p<0.0001$) Hsp70 mRNA expression more than the less specific inhibitor quercetin ($p=0.01$; Figure 14. A).

According to the resazurin viability assay, the *in vitro* mEHT treatment of 4T1 cells in combination with the HSR inhibitors resulted in significantly lower tumor cell viability 24 h post-treatment (Figure 14. B). KRIBB11 was able to reduce viability significantly already in monotherapy, suggesting that the more specific and more powerful inhibition of the heat shock machinery of the cells can be effective in itself in inducing tumor cell death (Figure 14. B). Combined treatment of the HSR inhibitors with mEHT resulted in a synergistic effect, as both combinations lead to significantly lower viability than the sum of the viability losses due to the two single therapies applied individually (significance of interaction: $p=0.0001$; Figure 14. A).

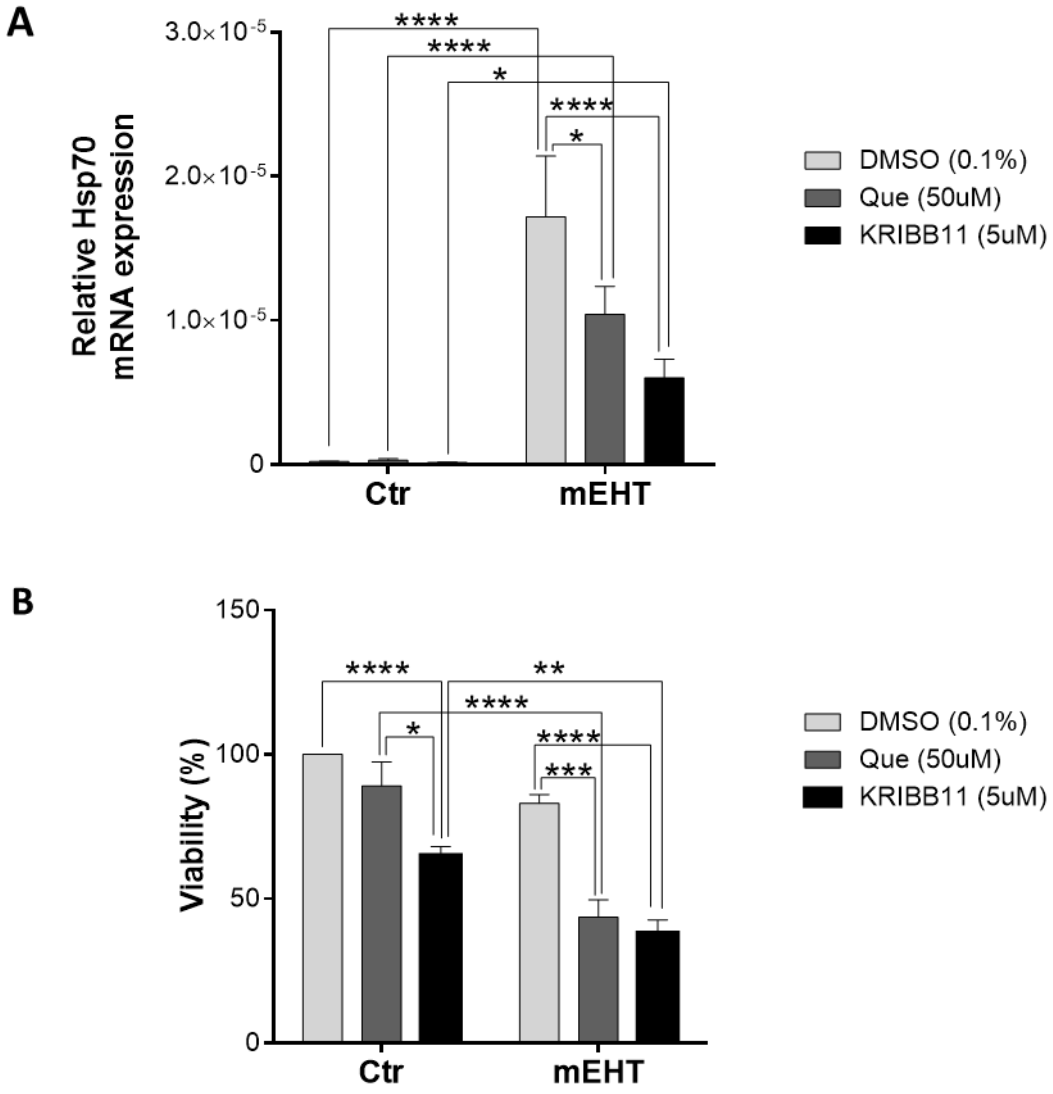

Figure 14. Synergistic effect of mEHT and heat shock inhibitors 4T1 cells pre-treated with heat shock response inhibitors, quercetin (Que) or KRIBB11, or vehiculum (DMSO) for 1 h before mEHT (42 °C, 30 min) treatment. (**A**) Hsp70 mRNA 2 h post-mEHT, normalized to 18S rRNA. (**B**) Resazurin viability assay, 24 h post-mEHT, viability expressed as percent of DMSO control (37 °C, vehiculum only). Two-way ANOVA, Mean ± SEM, n = 5–12/group, * $p < 0.05$, ** $p < 0.01$, *** $p < 0.001$, **** $p < 0.0001$ [18].

4. Discussion

The mEHT treatment of the orthotopic mammary tumors of mice was not feasible with the previously used LabEHY-100 preclinical mEHT device with tissue electrode for small animal treatment. Therefore, our research group participated in the development of an improved preclinical device and electrode optimized for treating inguinal mammary tumors to be able to investigate the effects of mEHT on a triple-negative breast cancer model. The new preclinical mEHT setup – LabEHY-200 device with the ergonomically designed pole electrode – was introduced at the first time by our research group [18]. This new setup allowed highly selective tumor treatment as detected by selective warming of the tumor tissue. The core temperature of the tumors was 2.5 ± 0.5 °C higher compared to the skin temperature above the tumor. The temperature gradient was reproducible and constant during treatments. Others reported comparable temperature gradients between the core of the tumors and the skin above the tumor using the former preclinical mEHT treatment setup under similar treatment conditions in other tumor types [116–118]. Thus, we concluded that the newly developed preclinical mEHT setup was successfully optimized for treating mouse mammary tumors in the inguinal region, which could not be achieved before. The other notable benefit of the highly reproducible and constant temperature gradients during treatments was that invasive temperature recording of the tumors – insertion of a temperature sensor into the core of the tumor – was not necessary, since we validated that the skin temperature can precisely and reliably indicate the estimated temperature of the tumors. Thus, we could conduct the temperature follow-up in a non-invasive way, and could therefore exclude the bias and side effects (bleeding, infection, tumor dissemination) caused by invasive puncturing of the tumors with the thermal probe.

The selective increase of tumor temperature is a specific feature of modulated electro-hyperthermia, since heat accumulation with whole-body hyperthermia or non-modulated radiofrequency induced capacitive hyperthermia approaches generally do not allow $\Delta T > 1$ °C, due to altered vascularization of tumors, which result in highly variable heating [26,119,120].

The energy trap hypothesis proposes that the energy communicated during mEHT treatment is absorbed predominantly in the most hypoxic areas of the tumors. These are

less perfused hypoxic regions, which have lower impedance because of the accumulated acidic metabolites (e.g. lactic acid) compared to normoxic tissues, thus the current density induced by RF is larger in the hypoxic parts of the tumors [24]. Furthermore, the lower perfusion results in heat trapping, as the heat dissipation by the circulation of the tumor is significantly reduced. In our case this theory is supported by the observation of destruction in the cores of the tumors, as hypoxia is usually most pronounced in the central area of the tumors, because it is vascularized the least [121].

Furthermore, an important reason for the highly effective and selective heating and killing of the tumor by mEHT is amplitude modulation (AM) and its non-thermal effects on the tumor cells. In addition to the thermal effect of the dielectric heating by the 13.56 MHz carrier frequency, the non-thermal effects result in much more extensive tumor destruction than expected from non-modulated radiofrequency capacitive hyperthermia [122–124]. The non-thermal effects are also demonstrated in cell culture experiments, where mEHT treatment was compared with conventional radiation heating to similar temperatures [122,125].

One of the most commonly used parameters to characterize hyperthermia treatments in biological models as well as in clinical practice is the specific absorption rate (SAR), which is the mass-normalized rate of energy-absorption (W/kg) by a biological material [126]. The SAR can be calculated from the dynamics of temperature rise during the initial heating-up period of the hyperthermia treatment [126].

$$SAR = \Delta T \times C/t$$

(ΔT: temperature gradient, C: specific heat of the biological material [J/K*kg], t: time [s])

In our experiments, the temperature rise was around 1.5 °C/minute in the pre-heating period, corresponding to a SAR of ~90 W/kg achieved in the tumors, which is higher than the usual SAR (30–40 W/kg) in clinical use [127]. However, in some cases documented by Griffiths *et al.*, SAR values even as high as 89 W/kg – which is comparable to the SAR in our experiment – could be achieved during human hyperthermia treatments, mostly in superficial tumors [128]. The bigger size of human tumors may also contribute to the explanation why SAR values are lower in clinical practice than in our mouse experiment, as larger tumors need lower SAR to achieve the same temperature, due to the

inverse relationship between the SAR value and the weight of the biological material. Nevertheless, in the case of modulated electro-hyperthermia the standard way of SAR calculation (see formula above) may be misleading, as during mEHT the energy is absorbed by lipid rafts of the tumor cell membranes (nanoheating) and this leads to the warming up of the whole tumor [124,129]. Thus, the actual weight of the heated target (lipid rafts) is much lower than the weight of the tumor. As a result, the estimated value of SAR in the case of mEHT is ~1 kW/kg, which corresponds to nanoparticle heating, and the heating is heterogeneous [130]. As SAR calculation is dependent on the weight of the heated target as well as on the average temperature of the target, its usefulness for the definition of the thermal parameters of mEHT treatment is limited [124].

During mEHT treatment, the energy absorption in the tumor causes cell stress and initiates the expression of cell stress-associated molecules [131]. One of the most abundant stress-induced molecules is Hsp70, which becomes strongly overexpressed in response to heat stress and damage [132]. Hsp70 has ambivalent effects on tumor progression as it can mediate both tumor-promoting and tumor-suppressing pathways, depending on its macroscopic (tumor cells or tumor stroma) and microscopic (intracellular, membrane-bound or extracellular) localization [99,133]. Hsp70 overexpression is a common feature of tumor cells and in several cancer types – including breast cancers [134,135] – the expression level of Hsp70 correlates with cancer aggressiveness and disease progression [133]. However, in certain malignancies Hsp70 expression even indicates good prognosis or improved therapeutic response [136–138].

Not just tumor cells, but cells of the tumor stroma can also express remarkable level of Hsp70 [139]. Tumor stroma is becoming more and more the focus of cancer research, as it seems to play a crucial role in tumor progression. However, these mechanisms are not yet sufficiently explored [140]. It is already known that expression of Hsp70 by stromal cells can be a key tumor-promoting factor and it is often essential in supporting tumor growth, thus its inhibition can serve as a potential therapeutic target [139]. However, Hsp70 has a “Janus face”, as membrane-bound or extracellular expression of Hsp70 can mediate anti-tumor mechanisms [118,133,141]. Juhasz *et al.* provide a detailed description of the tumor-suppressing effects of extracellular Hsp70, which acts as a danger signal and induces the activation of the immune system against the tumor cells [133]. But they also noted the controversial role of Hsp70 in tumor progression, as the

above mentioned tumor-promoting function of Hsp70 has also been described [133]. In our experiments – as in the literature – 4T1 tumors had very poor immunogenicity and very low rate of tumor-infiltrating immune cells called as an immune-desert or non-inflamed phenotype. According to our unpublished findings and literature data [142], we assumed that the immune cell-mediated tumor-suppressing effects induced by Hsp70 may be negligible in the 4T1 model. This was confirmed by the fact that inhibiting Hsp70 *in vitro* with quercetin or KRIBB11 significantly augmented the tumor-destructive effect of mEHT (discussed in detail later). It has been reported that mEHT provoked Hsp70 overexpression in HepG2 hepatic [143], B16F10 melanoma [118], and CT26 colorectal [144,145] cancer cells after mEHT treatment *in vitro* and in B16F10 (melanoma) [118], CT26 [146] and HT29 [147] (both colorectal) tumors *in vivo*. Similarly, we also found that mEHT treatments induced substantial damage in the core of the TNBC tumors surrounded by extensive Hsp70 expression. The central damage and the Hsp70-positive "ring" around the dead area supports the assumption that (i) mEHT heated the tumor centrally, in consequence of the heat and energy trap phenomena (discussed earlier) and that (ii) tumor destruction started in the core of the tumor and progressed outward. The cells surrounding the damaged area must have been exposed to severe stress by mEHT, but the high Hsp70 expression could protect them from cell death. The lack of similarly strong staining in sham-treated tumors demonstrates the specific Hsp70-inducing effect of mEHT. The time kinetic experiment demonstrated that Hsp70 mRNA peaked already 4 h post-treatment, followed by a peak of Hsp70 protein at 12 h post-treatment. Andocs *et al.* also reported similar dynamics of Hsp70 mRNA changes after mEHT treatment [147]. As Hsp70 protein returned close to sham level at 24 h, we observed tumor cell death marked by cleaved caspase-3 positivity, suggesting that exhaustion of Hsp70-mediated protection led to apoptotic cell death. Our findings are in good agreement with the literature, as Hsp70 has been demonstrated to inhibit caspase-mediated apoptosis [133,148]. The mEHT-induced tumor cell destruction is a long-lasting effect, as TDR was still significantly higher in mEHT-treated tumors 72 h post-treatment compared to sham. Previous reports support that mEHT induces caspase-3 activation (i.e. cleavage) *in vitro* in human ovarian (OVCAR-3), cervical (SNU-17) [149], and mouse colorectal (CT26) [146] carcinoma cells. The cleaved caspase-3 expression also increased in CT26 cells *in vivo* as a result of mEHT monotherapy [144,146]. However, we demonstrated for the first

time that mEHT first activates the protective machinery (i.e. Hsp70 induction), and then, as a consequence of the exhaustion of these protective mechanisms, cells undergo caspase-3-mediated cell death. Although we cannot exclude necrotic and other forms of cell death, the cC3 positivity of the dead area as well as the lack of morphological signs of necrotic cells on hematoxylin and eosin stained sections, such as pale or absent nuclei or hypereosinophilia of the cytoplasm, suggest that the dominant form of cell death was apoptosis.

The tumor-cell-killing effect of mEHT and the consequent reduction in viable tumor cell count have already been demonstrated in several *in vitro* experiments using other cell lines, such as U87-MG and A172 human glioma cells [150], OVCAR-3, SK-OV-3, HeLa, and SNU-17 human ovarian and cervical cancer cells [149], CT26 colorectal carcinoma cells [144] and B16F10 mouse melanoma cells [118]. However, the acute viability-reducing ability of mEHT treatment has not yet been confirmed with imaging techniques *in vivo*. Furthermore, mEHT therapy has not been investigated before in any TNBC mouse model, possibly due to the lack of appropriate tools. Our study demonstrated a significant reduction of viable tumor cell numbers *in vivo* already after two mEHT treatments in monotherapy. The decrease in viable cell count, as detected by IVIS imaging *in vivo*, was corroborated by determination of the tumor destruction ratio on hematoxylin-eosin-stained sections and hypocellularity by Ki67 immunostaining. The area of tumor destruction was cleaved caspase-3-positive, suggesting apoptotic cell death. We were not able to confirm tumor size reduction using conventional and less sensitive tumor size measuring methods such as the digital caliper and the ultrasound after 2 treatments. The most likely explanation for this deficiency is that the apoptotic/damaged tumor area (detected as TDR on the histology sections) had not yet been removed by the immune system during the short follow-up period. We confirmed this hypothesis on histology examinations so as another study by our team [23] with longer follow-up, where tumor cell death also manifested in a significant tumor size reduction after five mEHT treatments.

Ki67 is a proliferation marker, as its expressed throughout the cell cycle from G1 to M-phase [151]. Elevated expression of Ki67 has been associated with poor prognosis in numerous cancer types, including breast cancer [152–157]. In breast cancers the Ki67 index – the fraction of Ki67-positive tumor cells – is used as a prognostic marker, and it

is also important in the molecular characterization of these malignancies [2,154,157]. In triple negative breast cancers the Ki67 index is usually very high, in fact, the highest in all molecular subtypes [2,157]. The high Ki67 index contributes to fast disease progression, higher rate of relapse and inferior survival [157]. In the present study, just two mEHT treatments did not reduce Ki67 mRNA and protein. However, five consecutive mEHT treatments were already able to significantly reduce Ki67 protein levels in our tumor model as assessed by immunohistochemistry [23]. Furthermore, the reduced density of viable tumor cells in histological sections also suggests reduced proliferation activity of mEHT-treated tumor cells as also detected by IVIS. Similarly, Thomas *et al.* presented significant reduction in Ki67 expression of B16F10 metastatic tumor nodules after six consecutive mEHT treatments of melanoma lung metastases *in vivo* [158].

We described modulated electro-hyperthermia-induced Hsp70 dynamics in our triple negative breast cancer model. Proper timing of treatments is extremely important to find the most vulnerable window for optimal effects. Based on our data, the maximized impact of mEHT can be expected with the application of the treatments every other day (at 48h intervals), as the protective machinery (i.e. Hsp70 overexpression) is exhausted by 48h post-treatment, whereas the tumor tissue damage is still extensive at this time point.

We also demonstrated that the anti-tumor effect of mEHT can be enhanced by inhibiting the Hsp70-mediated defense mechanisms of tumor cells *in vitro*. Moreover, according to the paper by Gabai *et al.*, Hsp70 inhibitors may also diminish Hsp70 activation in the tumor stroma, and thus they can also abrogate the tumor-promoting microenvironment [139]. Using quercetin as a sensitizer to conductive hyperthermia (carried out in a regular water bath) was first described in 1984 by Kim *et al.* on HeLa cells and they interpreted its sensitizing effect on hyperthermia through the inhibition of lactate transport [159]. Since then, the synergistic effect of quercetin with conductive hyperthermia has been demonstrated in leukemic cells [160], melanoma cells [161], and prostate cancer [162], as a result of Hsp70 inhibition in all three cases. We demonstrated *in vitro* for the first time that quercetin was able to diminish the induction of Hsp70 mRNA upon capacitive hyperthermia (using mEHT technology) in 4T1 cells, to synergistically potentiate mEHT treatment. However, we have to note that the quercetin concentration (50 μM = 15 μg/mL) used in the *in vitro* experiments is much higher than

the steady state plasma concentration (~0,1 – 0,5 μg/mL) in patients after quercetin administration [163,164]. However, the plasma concentration of quercetin in humans can cover a very wide range (even up to 500 μg/mL) depending on dosage and way of administration [165]. According to the investigations of Ferry *et al.* the concentration of quercetin used in our model corresponds to patients' plasma concentrations 1 h after intravenous administration of extremely high quercetin doses: 25–50 mg/kg = 945–1700 mg/m^2; at doses of such magnitude, however, serious side effects may occur [165]. Besides, quercetin has very poor solubility, stability and bioavailability, thus its clinical use as HSR inhibitor in humans is rather limited [166]. Our *in vitro* model of the combined treatment using mEHT and quercetin served as the proof of principle for using an HSR inhibitor as a sensitizer to modulated electro-hyperthermia.

Based on our findings, we hypothesized that a more specific and more effective inhibitor of the Hsp70 machinery, KRIBB11 could enhance the tumor-killing effect of mEHT even more efficiently. Quercetin – besides its above mentioned unfavorable properties – is quite pleiotropic in mechanisms of action, and its Hsp70 inhibitory effect is the consequence of the indirect inhibition of Hsf-1 by blocking its hyperphosphorylation and thus its activation [109,111]. Since Hsf-1 is the central regulator of the cellular heat shock response, its more direct and specific blockade could lead to enhanced synergism with mEHT [110]. Therefore, we combined mEHT with the novel direct Hsf-1 inhibitor, KRIBB11. This molecule was introduced in 2011 by Yoon *et al.* as a highly effective Hsp70 synthesis inhibitor, as it binds directly to Hsf-1 and abolishes its Hsp70-promoting activity very specifically [167,168]. In the past few years, an increasing number of articles have been published about KRIBB11; however, it hasn't been investigated yet as a sensitizer to hyperthermia. We report for the first time, that KRIBB11 can be effectively combined with hyperthermia treatment, based on its Hsp70-inhibitory effect. The synergism of mEHT with Hsp70 inhibition should be confirmed and the pharmacokinetics and bioavailability of KRIBB11 should be determined in humans, as such data are not yet available. Our results suggest that inhibition of Hsp70 synergizes with modulated electro-hyperthermia and thus could enhance the anti-cancer therapeutic effects of mEHT.

5. Conclusion

The studies summarized in this thesis aimed to investigate the effects of modulated electro-hyperthermia in a triple-negative breast cancer animal model *in vitro* and *in vivo*. As a conclusion, our novel findings can demonstrate, that:

- a newly developed preclinical mEHT treatment device (LabEHY-200) could be optimized for treating orthotopic mammary tumors of small animals
- highly reproducible treatments could be performed with the optimized LabEHY-200 device *in vivo*
- highly effective and selective heating of the tumors could be achieved by mEHT treatments *in vivo*
- repeated mEHT treatments decreased the number of viable tumor cells *in vivo*
- repeated mEHT induced significant destruction of the tumors *in vivo*
- mEHT induced hypocellularity of the tumors already after two treatments *in vivo*
- mEHT inhibited proliferation by decreasing Ki67 expression after five treatments *in vivo*
- repeated mEHT induced caspase-dependent apoptosis *in vivo*
- repeated mEHT provoked Hsp70 overexpression *in vivo*
- the tumor destructive effect of mEHT is time-dependent *in vivo*
- the tumor cell killing effect of mEHT can be enhanced by combination with heat shock inhibitors *in vitro*

6. Summary

Breast cancer is one of the leading causes of cancer-related death among women. One of the most aggressive type of breast cancers is triple-negative breast cancer (TNBC), which accounts for about 15% of all breast cancers and has a very poor prognosis. Triple-negative breast cancer is a special subtype of breast cancers, as it does not express any estrogen-, progesterone-receptors or HER2, thus targeted therapies cannot be used. For those patients, who are diagnosed with TNBC the only approved systematic treatment option is the highly toxic and non-selective chemotherapy. Further steps are needed to identify new therapeutic possibilities.

Modulated electro-hyperthermia (mEHT) is a novel complementary loco-regional antitumor therapy, which applies alternating electromagnetic field to communicate energy to the tumor. mEHT is a unique capacitive electromagnetic treatment modality, as it induces both thermal and non-thermal effects in the tumor by using amplitude modulation of the 13.56 MHz radiofrequency.

The experimental work summarized in this thesis aimed to investigate the effects of mEHT on TNBC by using a preclinical mEHT treatment device on a mouse model of TNBC. We inoculated 4T1 mouse triple-negative breast cancer cells orthotopically into immunocompetent female Balb/C mice to form isografts. The isografts were treated with mEHT two or more times with 48h intervals. Tumor size were followed by IVIS, caliper and ultrasound. After the last treatment the tumors were removed, weighted and processed for histological and qPCR analysis.

Our experiments demonstrated that the tumors could be heated up effectively and selectively by the improved rodent mEHT device and the ergonomic pole electrode, and the treatments were highly reproducible. The treatments had a significant tumor cell-killing effect testified by In Vivo Imaging (IVIS). This finding was confirmed by the histological analysis of hematoxylin- and eosin-stained sections, which showed significant tissue damage in the mEHT-treated tumors originating from the center of the tumors. The damaged areas showed prominent signs of apoptosis and pronounced cleaved caspase-3 positivity, indicating that mEHT induced apoptotic cell death in the tumors. The mEHT treatments provoked Hsp70 overexpression in the surviving tumor cells, implying the activation of the heat stress-related protective machinery of the tumor cells. This tumor-protecting mechanism was exhausted by 48h after the treatment. The effectivity of the mEHT treatments could be amplified significantly by combing mEHT with heat shock inhibitors – quercetin or KRIBB11 – *in vitro*. This finding has great translational potential.

7. References

[1] Bray, F., Ferlay, J., Soerjomataram, I., Siegel, R.L., Torre, L.A., and Jemal, A. (2018) Global cancer statistics 2018: GLOBOCAN estimates of incidence and mortality worldwide for 36 cancers in 185 countries. *CA: A Cancer Journal for Clinicians*. 68 (6), 394–424.

[2] Harbeck, N., Penault-Llorca, F., Cortes, J., Gnant, M., Houssami, N., Poortmans, P., Ruddy, K., Tsang, J., Cardoso, F. (2019) Breast cancer. *Nature Reviews Disease Primers*. 5 (1), 66.

[3] Cardoso, F., Senkus, E., Costa, A., Papadopoulos, E., Aapro, M., André, F., Harbeck, N., Aguliar Lopez, B., Barrios, C.H., Bergh, J., Biganzoli, L., Boers-Doets, C.B., Cardoso, M.J., Carey, L.A., Cortés, J., Curigliano, G., Die Ras, V., El Saglir, N. S., Eniu, A., Fallowfield, L., Francis, P. A., Gelmon, K., Johnston S. R.D., Kaufman, B., Koppikar, S., Krop, I.E., Mayer, M., Nakigudde, G., Offersen, B.V., Ohno, S., Pagani, O., Paluch-Shimon, S., Penault-Llorca, F., Prat, A., Rugo, H.S., Sledge, G.W., Spence, D., Thomssen, C., Vorobiof, D.A., Xu, B., Norton, L., Winer, E.P. (2018) 4th ESO-ESMO International Consensus Guidelines for Advanced Breast Cancer (ABC 4) †. *Annals of Oncology*. 29 (8), 1634-1657.

[4] Perou, C.M., Sørile, T., Eisen, M.B., Van De Rijn, M., Jeffrey, S.S., Ress, C.A., Pollack, J. R., Ross, D.T., Johnsen, H., Akslen, L. A., Fluge, Ø., Pergammenschikov, A., Williams, C., Zhu, S.X., Lønning, P.E., Børresen-Dale, A.L., Brown, P.O., Botstein, D. (2000) Molecular portraits of human breast tumours. *Nature*. 406 (6797), 747–752.

[5] Foulkes, W.D., Smith, I.E., Reis-Filho, J.S. (2010) Triple-Negative Breast Cancer. *New England Journal of Medicine*. 363 (20), 1938–1948.

[6] den Brok, W.D., Speers, C.H., Gondara, L., Baxter, E., Tyldesley, S.K., Lohrisch, C.A. (2017) Survival with metastatic breast cancer based on initial presentation, de novo versus relapsed. *Breast Cancer Research and Treatment*. 161 (3), 549–556.

[7] Badve, S., Dabbs, D.J., Schnitt, S.J., Baehner, F.L., Decker, T., Eusebi, V., Fox, S.B., Ichihara, S., Jacquemier, J., Lakhani, S.R., Palacios, J., Rakha, E.A., Richardson, A.L., Schmitt, F.C., Tan, P-H., Tse, G.M., Weigelt, B., Ellis, I.O., Reis-Filho, J.S. (2011) Basal-like and triple-negative breast cancers: a critical

review with an emphasis on the implications for pathologists and oncologists. *Modern Pathology*. 24 (2), 157–167.

[8] Bianchini, G., Balko, J.M., Mayer, I.A., Sanders, M.E., Gianni, L. (2016) Triple-negative breast cancer: Challenges and opportunities of a heterogeneous disease. *Nature Reviews Clinical Oncology*. 13 (11), 674–690.

[9] Kwa, M.J., Adams, S. (2018) Checkpoint inhibitors in triple-negative breast cancer (TNBC): Where to go from here. *Cancer*. 124 (10), 2086–2103.

[10] Senkus, E., Kyriakides, S., Ohno, S., Penault-Llorca, F., Poortmans, P., Rutgers, E., Zackrisson, S. (2015) Primary breast cancer: ESMO Clinical Practice Guidelines for diagnosis, treatment and follow-up † incidence and epidemiology. *Annals of Oncology*. 25 (Suppl 5), v8-30.

[11] Coates, A.S., Winer, E.P., Goldhirsch, A., Gelber, R.D., Gnant, M., Piccart-Gebhart, M.J., Thürlimann, B., Senn, H. J., André, F., Baselga, J., Bergh, J., Bonnefoi, H., Burstein, H., Cardoso, F., Castiglione-Gertsch, M., Colleoni, M., Curigliano, G., Davidson, N.E, Leo, A.D., Ejlersten, B., Forbs, J.F., Galimberti, V., Goodwin, P., Harbeck, N., Hayes, D.F., Huober, J., Hudis, C. A., Ingle, J.N., Jassem, J., Jiang, Z., Karlsson, P., Morrow, M., Orecchia, R., Kent Osborne, C., Partridge, A.H., de la Peña, L., Pritchard, K.I., Rutgers, E.J.T., Sedlmayer, F., Semiglazov, V., Shao, Z.M., Smith, I., Toi, M., Tutt, A., Viale, G., von Minckwitz, G., Watanabe, T., Whelan, T., Xu, B. (2015) Tailoring therapies-improving the management of early breast cancer: St Gallen International Expert Consensus on the Primary Therapy of Early Breast Cancer 2015. *Annals of Oncology*. 26 (8), 1533–1546.

[12] Petrelli, F., Borgonovo, K., Cabiddu, M., Lonati, V., Barni, S. (2012) Mortality, leukemic risk, and cardiovascular toxicity of adjuvant anthracycline and taxane chemotherapy in breast cancer: A meta-analysis. *Breast Cancer Research and Treatment*. 135 (2), 335–346.

[13] Marupudi, N.I., Han, J.E., Li, K.W., Renard, V.M., Tyler, B.M., Brem, H. (2007) Paclitaxel: A review of adverse toxicities and novel delivery strategies. *Expert Opinion on Drug Safety*. 6 (5), 609–621.

[14] Tao, J.J., Visvanathan, K., Wolff, A.C. (2015) Long term side effects of adjuvant chemotherapy in patients with early breast cancer. *Breast*. 24 (Suppl 2), S149–

S153.

[15] Ismail-Khan, R., Bui, M.M. (2010) A review of triple-negative breast cancer. *Cancer Control*. 17 (3), 173–176.

[16] Wahba, H.A., El-Hadaad, H.A. (2015) Current approaches in treatment of triple-negative breast cancer. *Cancer Biology and Medicine*. 12 (2), 106–116.

[17] Park, M.K., Lee, C.H., Lee, H. (2018) Mouse models of breast cancer in preclinical research. *Laboratory Animal Research*. 34 (4), 160.

[18] Danics, L., Schvarcz, C.A., Viana, P., Vancsik, T., Krenács, T., Benyó, Z., Kaucsár, T., Hamar, P. (2020) Exhaustion of protective heat shock response induces significant tumor damage by apoptosis after modulated electro-hyperthermia treatment of triple negative breast cancer isografts in mice. *Cancers*. 12 (9), 1–24.

[19] Aslakson, C.J., Miller, F.R. (1992) Selective events in the metastatic process defined by analysis of the sequential dissemination of subpopulations of a mouse mammary tumor. *Cancer Research*. 52 (6), 1399-1405

[20] Kaur, P., Nagaraja, G.M., Zheng, H., Gizachew, D., Galukande, M., Krishnan, S., Asea, A. (2012) A mouse model for triple-negative breast cancer tumor-initiating cells (TNBC-TICs) exhibits similar aggressive phenotype to the human disease. *BMC Cancer*. 12 (1), 120.

[21] Pulaski, B.A., Ostrand-Rosenberg, S. (2000) Mouse 4T1 Breast Tumor Model. *Current Protocols in Immunology*. 39 (1), 1934-3671.

[22] Pulaski, B.A., Ostrand-Rosenberg, S. (1998) Reduction of established spontaneous mammary carcinoma metastases following immunotherapy with major histocompatibility complex class II and B7.1 cell-based tumor vaccines. *Cancer Research*. 58 (7), 1486-1493.

[23] Schvarcz, C.A., Danics, L., Krenács, T., Viana, P., Béres, R., Vancsik, T., Nagy, Á., Gyenesei, A., Kun, J., Fonović, M., Vidmar, R., Benyó, Z., Kaucsár, T., Hamar, P. (2021) Modulated Electro-Hyperthermia Induces a Prominent Local Stress Response and Growth Inhibition in Mouse Breast Cancer Isografts. *Cancers*. 13 (7), 1744.

[24] Szasz, A., Szasz, N., Szasz, O. Oncothermia : principles and practices. *Springer Science*, Heidelberg. 2011: 173-390.

[25] Chicheł, A., Skowronek, J., Kubaszewska, M., Kanikowski, M. (2007) Hyperthermia – description of a method and a review of clinical applications. *Reports of Practical Oncology & Radiotherapy*. 12 (5), 267–275.

[26] Roussakow, S. (2013) The History of Hyperthermia Rise and Decline. *Conference Papers in Medicine*. 22, 1–40.

[27] Kaur, P., Hurwitz, M.D., Krishnan, S., Asea, A. (2011) Combined hyperthermia and radiotherapy for the treatment of cancer. *Cancers*. 3 (4), 3799–3823.

[28] Ohno, S., Siddik Z.H., Kido Y., Zwelling, L.A., Bull, J.M. (1994) Thermal enhancement of drug uptake and DNA adducts as a possible mechanism for the effect of sequencing hyperthermia on cisplatin-induced cytotoxicity in L1210 cells. *Cancer Chemotherapy and Pharmacology.* 34 (4), 302-306.

[29] Ponce, A.M., Vujaskovic Z., Yuan, F., Needham, D., Dewhirst, M.W., (2006) Hyperthermia mediated liposomal drug delivery. *International Journal of Hyperthermia.* 22 (3), 205-213.

[30] Hildebrandt, B., Hegewisch-Becker, S., Kerner, T., Nierhaus, A., Bakhshandeh-Bath, A., Janni, W., Zumschlinge, R., Sommer, H., Riess, H., Wust, P. (2005) Current status of radiant whole-body hyperthermia at temperatures >41.5°C and practical guidelines for the treatment of adults. The German "Interdisciplinary Working Group on Hyperthermia". *International Journal of Hyperthermia*. 21 (2), 169–183.

[31] Yang, W.-H., Xie, J., Lai, Z.-Y., Yang, M.-D., Zhang, G.-H., Li, Y., Mu, J-B., Xu, J. (2019) Radiofrequency deep hyperthermia combined with chemotherapy in the treatment of advanced non-small cell lung cancer. *Chinese Medical Journal*. 132 (8), 922–927.

[32] Feldmann, H.J., Molls, M., Heinemann, H.G., Romanowski, R., Stuschke, M., Sack, H. (1993) Thermoradiotherapy in locally advanced deep seated tumours - thermal parameters and treatment results. *Radiotherapy and Oncology*. 26 (1), 38–44.

[33] Bagshaw, M.A., Taylor, M.A., Kapp, D.S., Meyer, J.L., Samulski, T. V, Lee, E.R., Fessenden, P. (1984) Anatomical Site-specific Modalities for Hyperthermia. *Cancer Research*. 44 (Suppl 10), 4842s-4852s.

[34] Petrovich, Z., Langholz, B., Astrahan, M., Emami, B. (1988) Deep microwave

hyperthermia for metastatic tumors of the liver. *Recent Results in Cancer Research*. 107, 244–248.

[35] Tanaka, R., Kim, C.H., Yamada, N., Saito, Y. (1987) Radiofrequency Hyperthermia for Malignant Brain Tumors: Preliminary Results of Clinical Trials. *Neurosurgery*. 21 (4), 1–3.

[36] Van Rhoon, G.C. (1994) Radiofrequency hyperthermia systems, experimental and clinical assessment of the feasibility of radiofrequency hyperthermia systems for loco-regional deep heating, Doctoral Thesis, Delft University of Technology.

[37] Valdagni, R., Amichetti, M., Dell'Orsola, G. (1982) Local microwave hyperthermia in cancer therapy. Preliminary report. *Tumori*. 68 (3), 247–251.

[38] Ichinoseki-Sekine, N., Naito, H., Saga, N., Ogura, Y., Shiraishi, M., Giombini, A., Giovannini, V., Katamoto, S. (2008) Effects of microwave hyperthermia at two different frequencies (434 and 2450 MHz) on human muscle temperature. *Journal of Sports Science and Medicine*. 7 (1), 191–193.

[39] Ryan, T.P., Brace, C.L. (2017) Interstitial microwave treatment for cancer: historical basis and current techniques in antenna design and performance. *International Journal of Hyperthermia*. 33 (1), 3–14.

[40] Perez, C.A., Kopecky, W., Baglan, R., Rao, D.V., Johnson, R. (1981) Local Microwave Hyperthermia in Cancer Therapy: Preliminary report. *Henry Ford Hospital Medical Journal*. 29 (1), 16-23

[41] Luk, K.H., Purser, P.R., Castro, J.R., Meyler, T.S., Phillips, T.L. (1981) Clinical experiences with local microwave hyperthermia. *International Journal of Radiation Oncology, Biology, Physics*. 7 (5), 615–619.

[42] Colombo, R., Da Pozzo, L.F., Lev, A., Salonia, A., Rigatti, P., Leib, Z., Servadio, C., Calderera, E., Pavone-Macaluso, M. (1998) Local microwave hyperthermia and intravesical chemotherapy as bladder sparing treatment for select multifocal and unresectable superficial bladder tumors. *Journal of Urology*. 159 (3), 783–787.

[43] Yerushalmi, A., Fishelovitz, Y., Singer, D., Reiner, I., Arielly, J., Abramovici, Y., Catsenelson, R., Levy, E., Shani, A. (1985) Localized deep microwave hyperthermia in the treatment of poor operative risk patients with benign prostatic hyperplasia. *Journal of Urology*. 133 (5), 873–876.

[44] Yerushalmi, A., Shani, A., Fishelovitz, Y., Arielly, J., Singer, D., Levy, E.,

Katselson, R., Rakowsky, E., Stein, J.A. (1986) Local Microwave Hyperthermia in the Treatment of Carcinoma of the Prostate. *Oncology*. 43 (5), 299–305.

[45] Yerushalmi, A. (1988) Localized, non-invasive deep microwave hyperthermia for the treatment of prostatic tumors: the first 5 years. *Recent Results in Cancer Research.* 107, 141–146.

[46] Kaur, P., Aliru, M.L., Chadha, A.S., Asea, A., Krishnan, S. (2016) Hyperthermia using nanoparticles--Promises and pitfalls. *International Journal of Hyperthermia : The Official Journal of European Society for Hyperthermic Oncology, North American Hyperthermia Group*. 32 (1), 76–88.

[47] Giustini, A.J., Petryk, A.A., Cassim, S.M., Tate, J.A., Baker, I., Hoopes, P.J. (2010) Magnetic Nanoparticle Hyperthermia in Cancer Treatment. *Nano LIFE*. 1 (01n02), 17-32.

[48] Stauffer, P.R., Goldberg, S.N. (2004) Introduction: Thermal ablation therapy. *International Journal of Hyperthermia*. 20 (7), 671–677.

[49] https://oncotherm.hu/products/ehy-2030. *Date of download: 05.12.2020.*

[50] Morimoto, T., Kimura, S., Konishi, Y., Komaki, K., Uyama, T., Monden, Y., Kinouchi, Y., Iritani, T. (1993) A Study of the Electrical Bio-impedance of Tumors. *Journal of Investigative Surgery*. 6 (1), 25–32.

[51] Cheng, Y., Fu, M. (2018) Dielectric properties for non-invasive detection of normal, benign, and malignant breast tissues using microwave theories. *Thoracic Cancer*. 9 (4), 459–465.

[52] Alon, L., Sodickson, D.K., Deniz, C.M. (2016) Heat equation inversion framework for average SAR calculation from magnetic resonance thermal imaging. *Bioelectromagnetics*. 37 (7), 493–503.

[53] Vander Heiden, M.G., Cantley, L.C., Thompson, C.B. (2009) Understanding the Warburg Effect: The Metabolic Requirements of Cell Proliferation. *Science*. 324 (5930), 1029–1033.

[54] Parolini, I., Federici, C., Raggi, C., Lugini, L., Palleschi, S., De Milito, A., Coscia, C., Iessi, E., Logozzi, M, Molinari, A., Colone, M., Tatti, M., Sargiacomo, M., Fais, S. (2009) Microenvironmental pH is a key factor for exosome traffic in tumor cells. *The Journal of Biological Chemistry*. 284 (49), 34211-34222.

[55] Khramtsov, V.V., Gillies, R.J. (2014) Janus-faced tumor microenvironment and

redox. *Antioxidants & Redox Signaling*. 21 (5), 723–729.

[56] Head, J.F., Wang F., Lipari, C.A., Elliott, R.L. (2000) The important role of infrared imaging in breast cancer. *IEEE Engineering in Medicine and Biology Magazine*. 19 (3), 52–57.

[57] Gersing, E. (1999) Monitoring Temperature-Induced Changes in Tissue during Hyperthermia by Impedance Methodsa. *Annals of the New York Academy of Sciences*. 873 (1), 13–20.

[58] Damadian, R. (1971) Tumor detection by nuclear magnetic resonance. Science. 171 (3976), 1151-1153

[59] Zou, Y., Guo, Z. (2003) A review of electrical impedance techniques for breast cancer detection. *Medical Engineering and Physics*. 25 (2), 79-90.

[60] Fujita, S., Tamazawa M., Kuroda, K. (1998) Effects of blood perfusion rate on the optimization of RF-capacitive hyperthermia. *IEEE Transactions on Bio-Medical Engineering*. 45 (9), 1182-1186.

[61] Vaupel, P., Kallinowski, F., Okunieff, P. (1989) Blood Flow, Oxygen and Nutrient Supply, and Metabolic Microenvironment of Human Tumors: A Review. *Cancer Research*. 49 (23), 6449.

[62] Song C.W., Lokshina, A., Rhee, J.G., Patten, M., Levitt, S.H. (1984) Implication of blood flow in hyperthermic treatment of tumors. *IEEE Transactions on Bio-Medical Engineering*. 31 (1), 9-16.

[63] Dudar T.E., Jain, R.K. (1984) Differential response of normal and tumor microcirculation to hyperthermia. *Cancer Research*. 44 (2), 605-612.

[64] Song, C.W. (1984) Effect of local hyperthermia on blood flow and microenvironment: a review. *Cancer Research.* 44 (Suppl 10), 4721s-4730s.

[65] Keszler, G., Csapó Z., Spasokoutskaja, T., Sasvari-Székely, M., Virga, S., Demeter, A., Eriksson, S., Staub, M. (2000) Hyperthermy increase the phosphorylation of deoxycytidine in the membrane phospholipid precursors and decrease its incorporation into DNA. *Advances in Experimental Medicine and Biology*. 486, 333-337.

[66] Dikomey, E., Franzke, J. (1992) Effect of heat on induction and repair of DNA strand breaks in X-irradiated CHO cells. *International Journal of Radiation Biology*. 61 (2), 221–233.

[67] Nishida, T., Akagi K., Tanaka, Y. (1997) Correlation between cell killing effect and cell membrane potential after heat treatment: analysis using fluorescent dye and flow cytometry. *International Journal of Hyperthermia*. 13 (2), 227-234.

[68] Hodgkin, A.L., Katz, B. (1949) The effect of temperature on the electrical activity of the giant axon of the squid. *The Journal of Physiology*. 109 (1–2), 240–249.

[69] Ardenne, M., Lippmann, H., Reitnauer, P.G., Justus, J. (2004) Histological proof for selective stop of microcirculation in tumor tissue at pH 6.1 and 41 °C. *Naturwissenschaften*. 66, 59–60.

[70] Schwan, H.P. (1982) Nonthermal cellular effects of electromagnetic fields: AC-field induced ponderomotoric forces. *British Journal of Cancer*. 45 (Suppl. 5), 220–224.

[71] Pohl, H.A. (1951) The Motion and Precipitation of Suspensoids in Divergent Electric Fields. *Journal of Applied Physics*. 22 (7), 869–871.

[72] Teixeira-Pinto, A.A., Nejelski, L.L., Cutler, J.L., Heller, J.H. (1960) The behavior of unicellular organisms in an electromagnetic field. *Experimental Cell Research*. 20 (3), 548–564.

[73] Neumann, E., Rosenheck, K. (1972) Permeability changes induced by electric impulses in vesicular membranes. *The Journal of Membrane Biology*. 10 (1), 279–290.

[74] Zimmermann, U., Pilwat, G., Riemann, F. (1974) Dielectric Breakdown of Cell Membranes. *Biophysical Journal*. 14 (11), 881–899.

[75] Astumian, R.D. (2011) Stochastic conformational pumping: A mechanism for free-energy transduction by molecules. *Annual Review of Biophysics*. 40 (1), 289–313.

[76] Robertson, B., Astumian, R.D. (1990) Michaelis-Menten equation for an enzyme in an oscillating electric field. *Biophysical Journal.* 58 (4), 969-974.

[77] Blank, M., Goodman, R. (2011) DNA is a fractal antenna in electromagnetic fields. *International Journal of Radiation Biology*. 87 (4), 409–415.

[78] Blank, M., Goodman, R. (2009) Electromagnetic fields stress living cells. *Pathophysiology*. 16 (2–3), 71–78.

[79] Kirson, E.D., Gurvich, Z., Schneiderman, R., Dekel, E., Itzhaki, A., Wasserman, Y., Schatzberger, R., Palti, Y. (2004) Disruption of Cancer Cell Replication by

Alternating Electric Fields. *Cancer Research*. 64 (9), 3288–3295.

[80] Kirson, E.D., Dbalý, V., Tovarys, F., Vymazal, J., Soustiel, J.F., Itzhaki, A., Mordechovich, D., Steinberg-Shapira, S., Gurvich, Z., Schneiderman, R., Wasserman, Y., Salzberg, M., Ryffel, B., Goldsher, D., Dekel, E., Palti, Y. (2007) Alternating electric fields arrest cell proliferation in animal tumor models and human brain tumors. *Proceedings of the National Academy of Sciences of the United States of America*. 104 (24), 10152–10157.

[81] Barbault, A., Costa, F.P., Bottger, B., Munden, R.F., Bomholt, F., Kuster, N., Pasche, B. (2009) Amplitude-modulated electromagnetic fields for the treatment of cancer: Discovery of tumor-specific frequencies and assessment of a novel therapeutic approach. *Journal of Experimental and Clinical Cancer Research*. 28 (1), 51.

[82] Pareilleux, A., Sicard, N. (1970) Lethal effects of electric current on Escherichia coli. *Applied Microbiology*. 19 (3), 421–424.

[83] Richter, K., Haslbeck, M., Buchner, J. (2010) The Heat Shock Response: Life on the Verge of Death. *Molecular Cell*. 40 (2), 253–266.

[84] Ritossa, F. (1962) A new puffing pattern induced by temperature shock and DNP in drosophila. *Experientia*. 18 (12), 571–573.

[85] Ashburner, M., Bonner, J.J. (1979) The induction of gene activity in drosophila by heat shock. *Cell*. 17 (2), 241–254.

[86] Courgeon, A.M., Maisonhaute, C., Best-Belpomme, M. (1984) Heat shock proteins are induced by cadmium in Drosophila cells. *Experimental Cell Research*. 153 (2), 515–521.

[87] Heikkila, J.J., Schultz, G.A., Iatrou, K., Gedamu, L. (1982) Expression of a set of fish genes following heat or metal ion exposure. *The Journal of Biological Chemistry*. 257 (20), 12000–12005.

[88] Michel, G.P., Starka, J. (1986) Effect of Ethanol and Heat Stresses on the Protein Pattern of Zymomonas mobilis. *Journal of Bacteriology*. 165 (3), 1040-1042.

[89] Welch, W.J., Suhan, J.P. (1986) Cellular and biochemical events in mammalian cells during and after recovery from physiological stress. *Journal of Cell Biology*. 103 (5), 2035–2052.

[90] Welch, W.I., Suhan, J.P. (1985) Morphological study of the mammalian stress

response: Characterization of changes in cytoplasmic organelles, cytoskeleton, and nucleoli, and appearance of intranuclear actin filaments in rat fibroblasts after heat-shock treatment. *Journal of Cell Biology*. 101 (4), 1198–1211.

[91] Szalay, M.S., Kovács, I.A., Korcsmáros, T., Böde, C., Csermely, P. (2007) Stress-induced rearrangements of cellular networks: Consequences for protection and drug design. *FEBS Letters*. 581 (19), 3675–3680.

[92] Patriarca, E.J., Maresca, B. (1990) Acquired thermotolerance following heat shock protein synthesis prevents impairment of mitochondrial ATPase activity at elevated temperatures in Saccharomyces cerevisiae. *Experimental Cell Research*. 190 (1), 57–64.

[93] Vogel, J.L., Parsell, D.A., Lindquist, S. (1995) Heat-shock proteins Hsp104 and Hsp70 reactivate mRNA splicing after heat inactivation. *Current Biology*. 5 (3), 306–317.

[94] Yost, H.J., Lindquist, S. (1986) RNA splicing is interrupted by heat shock and is rescued by heat shock protein synthesis. *Cell*. 45 (2), 185–193.

[95] Boulon, S., Westman, B.J., Hutten, S., Boisvert, F.M., Lamond, A.I. (2010) The Nucleolus under Stress. *Molecular Cell*. 40 (2), 216–227.

[96] Buchan, J.R., Parker, R. (2009) Eukaryotic Stress Granules: The Ins and Outs of Translation. *Molecular Cell*. 36 (6), 932–941.

[97] Vigh, L., Nakamoto, H., Landry, J., Gomez-Munoz, A., Harwood, J.L., Horvath, I. (2007) Membrane regulation of the stress response from prokaryotic models to mammalian cells. *Annals of the New York Academy of Sciences*. 1113, 40-51.

[98] Zeuthen, E. (1971) Synchrony in Tetrahymena by heat shocks spaced a normal cell generation apart. *Experimental Cell Research*. 68 (1), 49–60.

[99] Nylandsted, J., Brand, K., Jäättelä, M. (2000) Heat shock protein 70 is required for the survival of cancer cells. *Annals of the New York Academy of Sciences*. 926, 122-125.

[100] Fulda, S., Gorman, A.M., Hori, O., Samali, A. (2010) Cellular stress responses: cell survival and cell death. *International Journal of Cell Biology*. 2010, 214074.

[101] Ciocca, D.R., Calderwood, S.K. (2005) Heat shock proteins in cancer: Diagnostic, prognostic, predictive, and treatment implications. *Cell Stress and Chaperones*. 10 (2), 86–103.

[102] Voellmy, R., Boellmann, F. (2007) Chaperone regulation of the heat shock protein response. *Advances in Experimental Medicine and Biology*. 594, 89–99.

[103] Vargas, A.J., Burd, R. (2010) Hormesis and synergy: Pathways and mechanisms of quercetin in cancer prevention and management. *Nutrition Reviews*. 68 (7), 418–428.

[104] Tang, S.M., Deng, X.T., Zhou, J., Li, Q.P., Ge, X.X., Miao, L. (2020) Pharmacological basis and new insights of quercetin action in respect to its anti-cancer effects. *Biomedicine and Pharmacotherapy*. 121, 109604.

[105] D'Andrea, G. (2015) Quercetin: A flavonol with multifaceted therapeutic applications? *Fitoterapia*. 106, 256–271.

[106] Li, Y., Yao, J., Han, C., Yang, J., Chaudhry, M.T., Wang, S., Liu H., Yin, Y. (2016) Quercetin, inflammation and immunity. *Nutrients*. 8 (3), 167.

[107] Hosokawa, N., Hirayoshi, K., Kudo, H., Takechi, H., Aoike, A., Kawai, K., Nagata, K. (1992) Inhibition of the activation of heat shock factor in vivo and in vitro by flavonoids. *Molecular and Cellular Biology*. 12 (8), 3490–3498.

[108] Nagai, N., Nakai, A., Nagata, K. (1995) Quercetin suppresses heat shock response by down regulation of HSF1. *Biochemical and Biophysical Research Communications*. 208 (3), 1099–1105.

[109] De Billy, E., Powers, M. V., Smith, J.R., Workman, P. (2009) Drugging the heat shock factor 1 pathway: Exploitation of the critical cancer cell dependence on the guardian of the proteome. *Cell Cycle*. 8 (23), 3806–3808.

[110] Zheng, X., Krakowiak, J., Patel, N., Beyzavi, A., Ezike, J., Khalil, A.S., Pincus, D. (2016) Dynamic control of Hsf1 during heat shock by a chaperone switch and phosphorylation. *eLife*. 5, e18638.

[111] Cheng, S.C., Huang, W.C., Pang, J.H.S., Wu, Y.H., Cheng, C.Y. (2019) Quercetin inhibits the production of il-1β-induced inflammatory cytokines and chemokines in arpe-19 cells via the mapk and nf-κb signaling pathways. *International Journal of Molecular Sciences*. 20 (12), 2957.

[112] Yoon, Y.J., Kim, J.A., Shin, K.D., Shin, D.S., Han, Y.M., Lee, Y.J., Lee, J.S., Kwon, B.-M., Han, D.C. (2011) KRIBB11 inhibits HSP70 synthesis through inhibition of heat shock factor 1 function by impairing the recruitment of positive transcription elongation factor b to the hsp70 promoter. *Journal of Biological*

Chemistry. 286 (3), 1737–1747.

[113] Antonietti, P., Linder, B., Hehlgans, S., Mildenberger, I.C., Burger, M.C., Fulda, S., Steinbach, J.P., Gessler, F., Rödel, F., Mittelbronn, M., Kögel, D. (2017) Interference with the HSF1/HSP70/BAG3 pathway primes glioma cells to matrix detachment and BH3 mimetic-induced apoptosis. *Molecular Cancer Therapeutics*. 16 (1), 156–168.

[114] Fok, J.H.L., Hedayat, S., Zhang, L., Aronson, L.I., Mirabella, F., Pawlyn, C., Bright, M.D., Wardell, C.P., Keats, J.J., De Billy, E., Rye, C.S., CHessum, N.E.A., Jones, K., Morgan, G.J., Eccles, S.A., Workman, P., Davies, F.E. (2018) HSF1 Is essential for myeloma cell survival and a promising therapeutic target. *Clinical Cancer Research*. 24 (10), 2395–2407.

[115] Porter, A.G., Jänicke, R.U. (1999) Emerging roles of caspase-3 in apoptosis. *Cell Death and Differentiation*. 6 (2), 99–104.

[116] Jeon, T.-W., Yang, H., Lee, C.G., Oh, S.T., Seo, D., Baik, I.H., Lee, E.H., Yun, I., Park, K.R., Lee, Y.-H. (2016) Electro-hyperthermia up-regulates tumour suppressor Septin 4 to induce apoptotic cell death in hepatocellular carcinoma. *International Journal of Hyperthermia*. 32 (6), 648–656.

[117] Qin, W., Akutsu, Y., Andocs, G., Suganami, A., Hu, X., Yusup, G., Komatsu-Akimoto, A., Hoshino, I., Hanari, N., Mori, M., Isozaki, Y., Akanuma, N., Tamura, Y., Matsubara, H. (2014) Modulated electro-hyperthermia enhances dendritic cell therapy through an abscopal effect in mice. *Oncology Reports*. 32 (6), 2373–2379.

[118] Besztercei, B., Vancsik, T., Benedek, A., Major, E., Thomas, M.J., Schvarcz, C.A., Krenács, T., Benyó, Z., Balogh, A. (2019) Stress-Induced, p53-Mediated Tumor Growth Inhibition of Melanoma by Modulated Electrohyperthermia in Mouse Models without Major Immunogenic Effects. *International Journal of Molecular Sciences*. 20 (16), 4019.

[119] Hiraoka, M., Jo, S., Akuta, K., Nishimura, Y., Takahashi, M., Abe, M. (1987) Radiofrequency capacitive hyperthermia for deep-seated tumors. I. Studies on thermometry. *Cancer*. 60 (1), 121–127.

[120] Hiraoka, M., Jo, S., Akuta, K., Nishimura, Y., Takahashi, M., Abe, M. (1987) Radiofrequency capacitive hyperthermia for deep-seated tumors. II. Effects of thermoradiotherapy. *Cancer*. 60 (1), 128–135.

[121] Chekkoury, A., Nunes, A., Gateau, J., Symvoulidis, P., Feuchtinger, A., Beziere, N., Ovsepian, S.V., Walch, A., Ntziachristot, V. (2016) High-Resolution Multispectral Optoacoustic Tomography of the Vascularization and Constitutive Hypoxemia of Cancerous Tumors. *Neoplasia*. 18 (8), 459–467.

[122] Wust, P., Kortüm, B., Strauss, U., Nadobny, J., Zschaeck, S., Beck, M., Stein, U., Ghadjar, P. (2020) Non-thermal effects of radiofrequency electromagnetic fields. *Scientific Reports*. 10 (1), 1–8.

[123] Wust, P., Ghadjar, P., Nadobny, J., Beck, M., Kaul, D., Winter, L., Zschaeck, S. (2019) Physical analysis of temperature-dependent effects of amplitude-modulated electromagnetic hyperthermia. *International Journal of Hyperthermia*. 36 (1), 1246–1254.

[124] SZasz, A. (2013) Challenges and Solutions in Oncological Hyperthermia. *Thermal Medicine*. 29 (1), 1–23.

[125] Andocs, G., Rehman, M.U., Zhao, Q.L., Tabuchi, Y., Kanamori, M., Kondo, T. (2016) Comparison of biological effects of modulated electro-hyperthermia and conventional heat treatment in human lymphoma U937 cells. *Cell Death Discovery*. 2 (1), 16039.

[126] Chou, C.K. (1990) Use of heating rate and specific absorption rate in the hyperthermia clinic. *International Journal of Hyperthermia*. 6 (2), 367–370.

[127] Kok, H.P., Schooneveldt, G., Bakker, A., de Kroon-Oldenhof, R., Korshuize-van Straten, L., de Jong, C.E., Steggerda-Carvalho, E., Geijsen, E.D., Stalpers, L.J.A., Crezee, J. (2018) Predictive value of simulated SAR and temperature for changes in measured temperature after phase-amplitude steering during locoregional hyperthermia treatments. *International Journal of Hyperthermia*. 35 (1), 330–339.

[128] Griffiths, H., Ahmed, A., Smith, C.W., Moore, J.L., Kerby, I.J., Davies, R.M.E. (1986) Specific absorption rate and tissue temperature in local hyperthermia. *International Journal of Radiation Oncology, Biology, Physics*. 12 (11), 1997–2002.

[129] Papp, E., Vancsik, T., Kiss, E., Szasz, O. (2017) Energy Absorption by the Membrane Rafts in the Modulated Electro-Hyperthermia (mEHT). *Open Journal of Biophysics*. 07 (04), 216–229.

[130] Dutz, S., Hergt, R. (2013) Magnetic nanoparticle heating and heat transfer on a

microscale: Basic principles, realities and physical limitations of hyperthermia for tumour therapy. *International Journal of Hyperthermia*. 29 (8), 790–800.

[131] Repasky, E., Issels, R. (2002) Physiological consequences of hyperthermia: heat, heat shock proteins and the immune response. *International Journal of Hyperthermia*. 18 (6), 486–489.

[132] Rosenzweig, R., Nillegoda, N.B., Mayer, M.P., Bukau, B. (2019) The Hsp70 chaperone network. *Nature Reviews Molecular Cell Biology*. 20 (11), 665-680.

[133] Juhasz, K., Lipp, A.M., Nimmervoll, B., Sonnleitner, A., Hesse, J., Haselgruebler, T., Balogi, Zs. (2014) The complex function of Hsp70 in metastatic cancer. *Cancers*. 6 (1), 42–66.

[134] Ciocca, D.R., Clark, G.M., Tandon, A.K., Fuqua, S.A.W., Welch, W.J., Mcguire, W.L. (1993) Heat shock protein hsp70 in patients with axillary lymph node-negative breast cancer: Prognostic implications. *Journal of the National Cancer Institute*. 85 (7), 570–574.

[135] Thanner, F., Sütterlin, M.W., Kapp, M., Rieger, L., Kristen, P., Dietl, J., Gassel, A.M., Müller, T. (2003) Heat-shock protein 70 as a prognostic marker in node-negative breast cancer. *Anticancer Research*. 23 (2A), 1057–1062.

[136] Trieb, K., Lechleitner, T., Lang, S., Windhager, R., Kotz, R., Dirnhofer, S. (1998) Heat shock protein 72 expression in osteosarcomas correlates with good response to neoadjuvant chemotherapy. *Human Pathology*. 29 (10), 1050–1055.

[137] Nakajima, M., Kato, H., Miyazaki, T., Fukuchi, M., Masuda, N., Fukai, Y., Sohda, M., Ahmad, F., Kuwano, H. (2009) Tumor Immune Systems in Esophageal Cancer with Special Reference to Heat-shock Protein 70 and Humoral Immunity. *Anticancer Research*. 29 (5), 1595-1606.

[138] Santarosa, M., Favaro, D., Quaia, M., Galligioni, E. (1997) Expression of heat shock protein 72 in renal cell carcinoma: Possible role and prognostic implications in cancer patients. *European Journal of Cancer Part A*. 33 (6), 873–877.

[139] Gabai, V.L., Yaglom, J.A., Wang, Y., Meng, L., Shao, H., Kim, G., Colvin, T., Gestwicki, J., Sherman, M.Y. (2016) Anticancer effects of targeting Hsp70 in tumor stromal cells. *Cancer Research*. 76 (20), 5926–5932.

[140] Bremnes, R.M., Dønnem, T., Al-Saad, S., Al-Shibli, K., Andersen, S., Sirera, R., Camps, C., Marinez, I., Busund, L.-T. (2011) The role of tumor stroma in cancer

progression and prognosis: Emphasis on carcinoma-associated fibroblasts and non-small cell lung cancer. *Journal of Thoracic Oncology*. 6 (1), 209–217.

[141] Komarova, E.Y., Marchenko, L. V., Zhakhov, A. V., Nikotina, A.D., Aksenov, N.D., Suezov, R. V., Ischenko, A.M., Margulis, B.A., Guzhova, I.V. (2020) Extracellular hsp70 reduces the pro-tumor capacity of monocytes/macrophages co-cultivated with cancer cells. *International Journal of Molecular Sciences*. 21 (1), 59.

[142] Lechner, M.G., Karimi, S.S., Barry-Holson, K., Angell, T.E., Murphy, K.A., Church, C.H., Ohlfest, J.R., Hu, P., Epstein, A.L. (2013) Immunogenicity of murine solid tumor models as a defining feature of in vivo behavior and response to immunotherapy. *Journal of Immunotherapy*. 36 (9), 477–489.

[143] Yang, K.-L., Huang, C.-C., Chi, M.-S., Chiang, H.-C., Wang, Y.-S., Hsia, C.-C., Andocs, G., Wang, H.-E., Chi, K.-H. (2016) In vitro comparison of conventional hyperthermia and modulated electro-hyperthermia. *Oncotarget*. 7 (51), 84082–84092.

[144] Vancsik, T., Forika, G., Balogh, A., Kiss, E., Krenacs, T. (2019) Modulated electro-hyperthermia induced p53 driven apoptosis and cell cycle arrest additively support doxorubicin chemotherapy of colorectal cancer in vitro. *Cancer Medicine*. 8 (9), 4292-4303.

[145] Tsang, Y.-W., Huang, C.-C., Yang, K.-L., Chi, M.-S., Chiang, H.-C., Wang, Y.-S., Andocs, G., Szasz, A., Li, W.-T., Chi, K.-H. (2015) Improving immunological tumor microenvironment using electro-hyperthermia followed by dendritic cell immunotherapy. *BMC Cancer*. 15 (1), 708.

[146] Vancsik, T., Kovago, C., Kiss, E., Papp, E., Forika, G., Benyo, Z., Meggyeshazi, N., Krenacs, T. (2018) Modulated electro-hyperthermia induced loco-regional and systemic tumor destruction in colorectal cancer allografts. *Journal of Cancer*. 9 (1), 41–53.

[147] Andocs, G., Meggyeshazi, N., Balogh, L., Spisak, S., Maros, M.E., Balla, P., Kiszner, G., Teleki, I., Kovago, Cs., Krenacs, T. (2015) Upregulation of heat shock proteins and the promotion of damage-associated molecular pattern signals in a colorectal cancer model by modulated electrohyperthermia. *Cell Stress & Chaperones*. 20 (1), 37–46.

[148] Nylandsted, J., Gyrd-Hansen, M., Danielewicz, A., Fehrenbacher, N., Lademann, U., Høyer-Hansen, M., Weber, E., Multhoff, G., Rohde, M., Jäättelä, M. (2004) Heat shock protein 70 promotes cell survival by inhibiting lysosomal membrane permeabilization. *Journal of Experimental Medicine*. 200 (4), 425–435.

[149] Yang, W., Han, G.H., Shin, H.-Y., Lee, E.-J., Cho, H., Chay, D.B., Kim, J.-H. (2019) Combined treatment with modulated electro-hyperthermia and an autophagy inhibitor effectively inhibit ovarian and cervical cancer growth. *International Journal of Hyperthermia*. 36 (1), 9–20.

[150] Cha, J., Jeon, T.-W., Lee, C.G., Oh, S.T., Yang, H.-B., Choi, K.-J., Seo, D., Yun, I., Baik, I.H., Park, K.R., Park, Y.N., Lee, Y.-H. (2015) Electro-hyperthermia inhibits glioma tumorigenicity through the induction of E2F1-mediated apoptosis. *International Journal of Hyperthermia*. 31 (7), 784–792.

[151] Scholzen, T., Gerdes, J. (2000) The Ki-67 protein: From the known and the unknown. *Journal of Cellular Physiology*. 182 (3), 311–322.

[152] Li, L.T., Jiang, G., Chen, Q., Zheng, J.N. (2015) Ki67 is a promising molecular target in the diagnosis of cancer. *Molecular Medicine Reports*. 11 (3), 1566–1572.

[153] Hammarsten, P., Josefsson, A., Thysell, E., Lundholm, M., Hägglöf, C., Iglesias-Gato, D., Flores-Morales, A., Stattin, P., Egevad, L., Granfors, T., Wikström, P., Bergh, A. (2019) Immunoreactivity for prostate specific antigen and Ki67 differentiates subgroups of prostate cancer related to outcome. *Modern Pathology*. 32 (9), 1310-1319.

[154] Soliman, N.A., Yussif, S.M. (2016) Ki-67 as a prognostic marker according to breast cancer molecular subtype. *Cancer Biology & Medicine*. 13 (4), 496–504.

[155] Melling, N., Kowitz, C.M., Simon, R., Bokemeyer, C., Terracciano, L., Sauter, G., Izbicki, J.R., Marx, A.H. (2016) High Ki67 expression is an independent good prognostic marker in colorectal cancer. *Journal of Clinical Pathology*. 69 (3), 209–214.

[156] Kanyilmaz, G., Benli Yavuz, B., Aktan, M., Karaagac, M., Uyar, M., Findik, S. (2019) Prognostic Importance of Ki-67 in Breast Cancer and Its Relationship with Other Prognostic Factors. *European Journal of Breast Health*. 15 (4), 256–261.

[157] Hashmi, A.A., Hashmi, K.A., Irfan, M., Khan, S.M., Edhi, M.M., Ali, J.P., Hashmi, S.K., Asif, H., Faridi, N., Khan, A. (2019) Ki67 index in intrinsic breast

cancer subtypes and its association with prognostic parameters. *BMC Research Notes*. 12 (1), 605.

[158] Thomas, M.J., Major, E., Benedek, A., Horváth, I., Máthé, D., Bergmann, R., Szász, A.M., Krenács, T., Benyó, Z. (2020) Suppression of metastatic melanoma growth in lung by modulated electro-hyperthermia monitored by a minimally invasive heat stress testing approach in mice. *Cancers*. 12 (12), 1–24.

[159] Kim, J.H., Kim, S.H., Alfieri, A.A., Young, C.W. (1984) Quercetin, an Inhibitor of Lactate Transport and a Hyperthermic Sensitizer of HeLa Cells. *Cancer Research*. 44 (1), 102-106.

[160] Piantelli, M., Tatone, D., Castrilli, G., Savini, F., Maggiano, N., Larocca, L.M., Ranelletti, F.O., Natali, P.G. (2001) Quercetin and tamoxifen sensitize human melanoma cells to hyperthermia. *Melanoma Research*. 11 (5), 469–476.

[161] Piantelli, M., Tatone, D., Castrilli, G., Savini, F., Maggiano, N., Larocca, L.M., Ranelletti, F.O., Natali, P.G. (2001) Quercetin and tamoxifen sensitize human melanoma cells to hyperthermia. *Melanoma Research*. 11 (5), 469–476.

[162] Asea, A., Ara, G., Teicher, B.A., Stevenson, M.A., Calderwood, S.K. (2001) Effects of the flavonoid drug Quercetin on the response of human prostate tumours to hyperthermia in vitro and in vivo. *International Journal of Hyperthermia*. 17 (4), 347–356.

[163] Riva, A., Ronchi, M., Petrangolini, G., Bosisio, S., Allegrini, P. (2019) Improved Oral Absorption of Quercetin from Quercetin Phytosome®, a New Delivery System Based on Food Grade Lecithin. *European Journal of Drug Metabolism and Pharmacokinetics*. 44 (2), 169–177.

[164] Jin, F., Nieman, D.C., Shanely, R.A., Knab, A.M., Austin, M.D., Sha, W. (2010) The variable plasma quercetin response to 12-week quercetin supplementation in humans. *European Journal of Clinical Nutrition*. 64 (7), 692–697.

[165] Ferry, D.R., Smith, A., Malkhandi, J., Fyfe, D.W., deTakats, P.G., Anderson, D., Baker, J., Kerr, D.J. (1996) Phase I clinical trial of the flavonoid quercetin: pharmacokinetics and evidence for in vivo tyrosine kinase inhibition. *Clinical Cancer Research*. 2 (4), 659-668.

[166] Wang, W., Sun, C., Mao, L., Ma, P., Liu, F., Yang, J., Gao, Y. (2016) The biological activities, chemical stability, metabolism and delivery systems of

quercetin: A review. *Trends in Food Science and Technology*. 56, 21–38.

[167] Yoon, Y.J., Kim, J.A., Shin, K.D., Shin, D.S., Han, Y.M., Lee, Y.J., Lee, J.S., Kwon, B.-M., Han, D.C. (2011) KRIBB11 inhibits HSP70 synthesis through inhibition of heat shock factor 1 function by impairing the recruitment of positive transcription elongation factor b to the hsp70 promoter. *Journal of Biological Chemistry*. 286 (3), 1737–1747.

[168] Shah, S.P., Lonial, S., Boise, L.H. (2015) When Cancer fights back: Multiple myeloma, proteasome inhibition, and the heat-shock response. *Molecular Cancer Research*. 13 (8), 1163–1173.

8. Bibliography of the candidate's publications

Publications related to the dissertation

Danics, L., Schvarcz, C.A., Viana, P., Vancsik, T., Krenács, T., Benyó, Z., Kaucsár, T., Hamar, P. (2020) Exhaustion of Protective Heat Shock Response Induces Significant Tumor Damage by Apoptosis after Modulated Electro-Hyperthermia Treatment of Triple Negative Breast Cancer Isografts in Mice. *Cancers (Basel)*. 12(9):2581. doi: 10.3390/cancers12092581. Impact factor: 6.639

Schvarcz, C.A., **Danics, L.**, Krenács, T., Viana, P., Béres, R., Vancsik, T., Nagy, Á., Gyenesei, A., Kun, J., Fonovič, M., Vidmar, R., Benyó, Z., Kaucsár, T., Hamar, P. (2021) Modulated electro-hyperthermia induces a prominent local stress response and growth inhibition in mouse breast cancer isografts. *Cancers (Basel)*. 13(7):1744. Doi: 10.3390/cancers13071744. Impact factor: 6.639

Publications not related to the dissertation

Bencze, N., Schvarcz, C.A., Kriszta, G., **Danics, L.,** Szőke, É., Balogh, P., Szállási, Á., Hamar, P., Helyes, Zs., Botz, B. (2021) Desensitization of capsaicin-sensitive afferents accelerates early tumor growth via increased vascular leakage in a murine model of triple negative breast cancer. *Frontiers in Oncology*. doi: 10.3389/fonc.2021.685297. Impact factor: 6.244

Dank, M., Balogh, A., Benedek, A., Besztercei, B., **Danics, L.,** Forika, G., Garay,T., Hamar, P., Karászi, Á., Kaucsár, T., Kiss, É., Krenács, T., Major, E., Mohácsi, R., Portörő, I., Ruisanchez, É., Schvarcz, Cs., Szász, A.M., Thomas, J.M., Vancsik, T., Zolcsák, Z., Benyó, Z. (2019) Elektromágneses daganatterápiás készülék preklinikai és klinikai vizsgálatai, valamint műszaki továbbfejlesztése: tapasztalatok szolid tumorokkal. *Magyar Onkológia*. 63(4):354-358.

9. Acknowledgement

I would like to thank my supervisor Professor Péter Hamar for his guidance and encouragement during the four years of my PhD studies. I am grateful for his professional advices and support of my research and publication.

I am also very thankful to Csaba András Schvarcz, my colleague and friend for being my partner in the experiments during the last four years. His efforts, support and help were indispensable; I could always count on him.

I would like to thank for the teaching and supervision to Tamás Kaucsár, who was a post-doctoral researcher in our research group in the first three years. His experience, precision and accuracy in research work served as a role model for me.

I would like to thank Tamás Vancsik for his efforts and help during the experiments, his knowledge and experience were essential for performing the experiments.

I am thankful to Professor Zoltán Benyó for providing the place and infrastructure for my research in the Institute of Translational Medicine and for his professional advices and support during my PhD studies.

I am also thankful for the supervision and support to Professor András Szász and I would also like to thank to the Oncotherm company for providing the Lab-EHY device and professional assistance.

I would like to express my sincere gratitude to all my co-authors for their effort, and all former and current colleagues at the Institute of Translational Medicine for their support.

I am truly thankful to Tibor Krenács for reviewing my thesis and my manuscripts, his professional remarks, suggestions and corrections contributed greatly to the improvement of my work.

Finally, I am very grateful to my parents, and to my whole family. Without their encouragement and support this thesis could not have been accomplished.